The Effect of a *PEX6* Mutation on Peroxisome Function

by

Matthew David Benson

A thesis submitted in partial fulfillment of the requirements for the degree of

Master of Science

Medical Sciences – Ophthalmology and Visual Sciences

University of Alberta

ABSTRACT

Purpose. Peroxisomal biogenesis disorders (PBDs) represent a group of recessive conditions that cause severe vision loss, sensorineural hearing loss, neurologic dysfunction, and other systemic abnormalities due to abnormal peroxisomal function. Appropriate therapies are needed as there are no disease-modifying treatments currently available for these conditions. Our lab identified a PBD in a 12-year old male with compound heterozygous mutations in *PEX6* (c.802_815del GACGGACTGGCGCT and c.35T>C (p.Phe12Ser)), resulting in congenital sensorineural hearing loss and retinopathy. Our study sought to examine the effect of mutations in *PEX6* on peroxisome metabolism to both enhance our understanding of disease mechanisms in peroxisomal disorders and to aid in identifying potential therapeutic interventions for these patients.

Methods. Patient-derived skin fibroblasts were grown in culture and a *PEX6* knock-out cell line was developed using CRISPR/Cas9 technology in HEK293T cells. The knock-out cell line was used to examine the effect of the complete absence of Pex6, recapitulating a more severe PBD phenotype, and to compare the results with those from the study of a patient's fibroblasts. Immunoblot analysis of whole cell lysates was performed to examine levels of endogenous Pex14, a marker of peroxisome abundance. Immunofluorescence studies were conducted using antibodies against components of the peroxisomal protein import pathway to interrogate the effects of changes in *PEX6* on protein

trafficking. Finally, we evaluated whether genetic approaches of over-expressing *PEX5*, the cytosolic shuttle for cargo destined for the peroxisomal matrix, and over-expressing *PEX6* would restore some peroxisome function in cells lacking Pex6.

Results. Endogenous levels of Pex14 were similar when comparing control fibroblasts to patient fibroblasts, suggesting that there was no gross defect in peroxisome abundance in our patient ($P = 0.64$). However, endogenous levels of Pex14 were less in *PEX6* knock-out cells compared to wild-type cells ($P = 0.04$), suggesting the presence of fewer peroxisomes. Immunofluorescence microscopy demonstrated significantly impaired PTS1- and PTS2-mediated matrix protein import in both patient fibroblasts and *PEX6* knock-out cells when compared to their respective controls. Over-expressing *PEX6*, but not *PEX5*, resulted in improved matrix protein import in *PEX6* knock-out cells.

Conclusions. Compound heterozygous mutations in *PEX6* are responsible for combined sensorineural hearing loss and retinopathy in our patient. In contrast to previous reports, the primary defect in our patient seems to be one of impaired peroxisomal protein import as opposed to a perturbation in overall peroxisome abundance. We postulate that this may be the mechanism of disease in patients with a milder PBD phenotype as a result of *PEX6* missense mutations and residual Pex6 protein. On the other hand, our *PEX6* knock-out cell data support a combination of reduced peroxisome abundance and impaired matrix protein import contributing to a severe PBD phenotype. Understanding the precise mechanism of disease at an individual patient level will be important in developing effective therapeutic strategies in the future.

PREFACE

This thesis is an original work by Matthew D. Benson. The research project, of which this thesis is a part, received research ethics approval from the University of Alberta Research Ethics Board, “Characterizing the Effect of a PEX6 Mutation on Peroxisome Structure and Function”, No. Pro00074451, December 11, 2017.

ACKNOWLEDGEMENTS

I would like to sincerely thank all of my mentors and role models for inspiring me and encouraging me to pursue my science and medicine interests. In particular, I would like to thank Dr. Thomas Simmen, Professor in Cell Biology, who first took me on as a research student in the summer of 2009. Dr. Simmen's lab was where my curiosity for research first began. My incredibly positive experience in Dr. Simmen's lab cultivated my inquisitive nature and nudged me towards pursuing a career in biomedical research.

In addition, I would like to thank Dr. Ordan Lehmann, Professor in Medical Genetics and Ophthalmology and Visual Sciences, who first introduced me to molecular genetics and ophthalmic research. Dr. Lehmann taught me how to effectively write a manuscript. I would also like to thank Dr. Richard Rachubinski, Professor in Cell Biology, for his advice and support for my thesis and for connecting me with other experts in peroxisome research.

I would also like to thank Dr. Ian MacDonald, Emeritus Professor in Ophthalmology and Visual Sciences, for all of the support and mentoring that he has kindly provided for me in both my research and clinical endeavors. He continues to instill in me a love for ocular genetics.

I would like to acknowledge Fighting Blindness Canada (FBC) for funding my research through a Clinician-Scientist Emerging Leader (CSEL) award.

Finally, I would like to thank my lab members, co-workers, co-residents, friends, and family for supporting me in my research efforts. I would like to especially thank Jen Ursella, my partner, for being so patient and understanding and for letting me squeeze in an extra hour or two of work each night.

TABLE OF CONTENTS

LIST OF TABLES

LIST OF FIGURES

LIST OF ABBREVIATIONS

AAA	ATPases Associated with Diverse Cellular Activities
CRISPR	Clustered Regularly Interspaced Short Palindromic Repeats
DHA	Docosahexanoic Acid
DMEM	Dulbecco's Modified Eagle Medium
DTM	Docking/Translocation Module
FBS	Fetal Bovine Serum
FACS	Fluorescence activated cell sorting
ffERG	Full Field Electroretinogram
GFP	Green Fluorescent Protein
HEK	Human Embryonic Kidney
IF	Immunofluorescence
iPSC	Induced Pluripotent Stem Cells
IRD	Inherited Retinal Dystrophy
LCA	Leber Congenital Amaurosis
NALD	Neonatal Adrenoleukodystrophy
OD	Oculus Dexter (Right Eye)
OS	Oculus Sinister (Left Eye)
OU	Oculus Uterque (Right and Left Eyes)

PBD	Peroxisomal Biogenesis Disorder
PBS	Phosphate Buffered Saline
PBS-T	Phosphate Buffered Saline with Tween-20
PCR	Polymerase Chain Reaction
PMP	Peroxisomal Membrane Protein
PTS1	Peroxisomal Targeting Signal-1
PTS2	Peroxisomal Targeting Signal-2
REM	Receptor/Exportomer Module
RGC	Retinal Ganglion Cell
RNP	Ribonucleoprotein
RP	Retinitis Pigmentosa
RPE	Retinal Pigment Epithelium
SD-OCT	Spectral Domain Optical Coherent Tomography
SNHL	Sensorineural Hearing Loss
VEGF	Vascular Endothelial Growth Factor
VLCFA	Very Long-Chain Fatty Acid
WB	Western Blot
WT	Wild-Type
ZSD	Zellweger Spectrum Disorders

INTRODUCTION

1. Vision and the Retina

1.1 Structure of the Retina

The human retina is a highly specialized tissue of neuroectodermal origin that facilitates the conversion of light energy into an electrochemical signal for vision. Structurally, the retina is composed of 10 unique layers that can be divided, more generally, into an outer retinal region and an inner retinal region (Figure 1). The outer retina, from outside-in, includes the retinal pigment epithelium (RPE), the rod and cone photoreceptors, the external limiting membrane, the outer nuclear layer, and the outer plexiform layer. These layers are nourished by blood vessels of the choriocapillaris, a superficial vascular layer derived from the choroid. The inner retina, from outside-in, includes the inner nuclear layer, inner plexiform layer, retinal ganglion cells, retinal nerve fiber layer, and the internal limiting membrane. The vascular supply to the inner retina arises from branches of the central retinal artery (Figure 1).

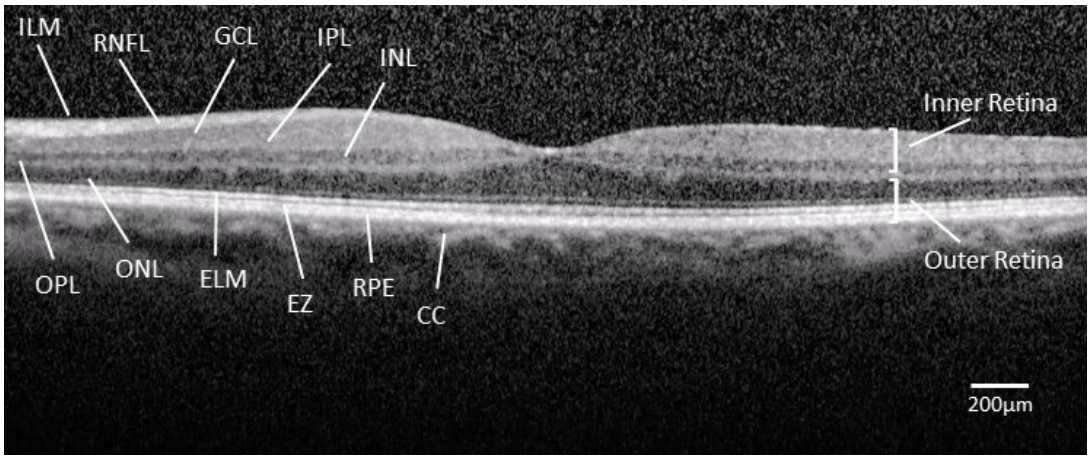

Figure 1. A spectral-domain optical coherence tomography (SD-OCT) image of a normal macula. The 10 characteristic layers of the retina are demonstrated and the choriocapillaris (CC) is highlighted as well. ILM = internal limiting membrane; RNFL = retinal nerve fiber layer; GCL = ganglion cell layer; IPL = inner plexiform layer; INL = inner nuclear layer; OPL = outer plexiform layer; ONL = outer nuclear layer; ELM = external limiting membrane; EZ = ellipsoid zone; RPE = retinal pigment epithelium; CC = choriocapillaris.

1.2 Outer Retina

The RPE exists as a monolayer of hexagonal cells linked by tight junctions and forms the outer blood-retinal barrier. This pigmented cell layer has been described as the "workhorse" of the retina[1] as it plays several critical roles. The presence of melanin within melanosomes in the RPE allows the cells to absorb excess light, protecting the retina from oxidative damage. The RPE also transports ions, water, and phototransduction by-products from the subretinal space and secretes growth factors, such as vascular endothelial growth factor (VEFG), to support the overlying photoreceptors and underlying choriocapillaris.[2] In addition to its role in maintaining an outer blood-retinal barrier, the RPE play an important role in innate immune responses.[3] A type of pattern recognition receptor called the toll-like receptor (TLR) is present in the RPE and responds to foreign material from viruses or bacteria, depending on the particular TLR subtype.[4] For example, TLR9 senses unmethylated CpG residues in the DNA from bacteria or viruses and responds by promoting the release of pro-inflammatory cytokines, including interleukin-8, from the RPE.[5] An understanding of the role of the RPE in innate immunity is guiding the development of viral vectors that minimally activate immune pathways in the retina with the goal of enhancing the efficacy of gene therapy.[6] Finally, the RPE cells contain apical microvilli that enable intimate connections with overlying photoreceptors. Phagocytosis of photoreceptor outer segments and enzymatic regeneration of the 11-cis-retinal chromophore are two key roles that the RPE plays in maintaining photoreceptors through the visual cycle.[2]

Photoreceptors are the light-sensitive elements of the outer retina and exist in two forms: rods and cones. Rods facilitate vision in dimly lit environments, whereas cones provide vision with

high resolution and color contrast. The general structure of the photoreceptor includes an outer segment, which interdigitates with RPE microvilli, a connecting cilium, an inner segment, cell body, and a synaptic terminal. The outer segments contain numerous discs or membrane evaginations and invaginations laden with visual pigment specific to the type of photoreceptor. Rods utilize rhodopsin as their visual pigment, whereas cones utilize one of three types of opsins, each with varying sensitivities to certain wavelengths of light (red, green, and blue opsins). A connecting cilium, which is a modified sensory cilium with 9+0 microtubule arrangement, links the outer segment with the inner segment that houses cellular organelles including mitochondria, Golgi, and ribosomes. The cell body contains the nucleus of the photoreceptor and defines the retinal outer nuclear layer. Finally, the synaptic terminal exists within the outer plexiform layer and this is the site where photoreceptors synapse with downstream bipolar cell axons.[7]

1.3 Inner Retina

Following the synapse between photoreceptors and bipolar cells in the outer plexiform layer, the inner nuclear layer is the location of the cell bodies of the bipolar cells, horizontal cells, and amacrine cells. Both horizontal and amacrine cells play roles in integrating signals between retinal neurons via feedback inhibition mechanisms.[8] The axons of the bipolar cells course through the inner plexiform layer where synapse occurs with retinal ganglion cells (RGCs). The cell bodies of the RGCs are located within the retinal ganglion cell layer and their axons form the retinal nerve fiber layer. Over one million of these neurons travel in the optic nerve where they eventually synapse intracranially at the lateral geniculate nucleus.[9]

2. Inherited Retinal Dystrophies (IRDs)

The inherited retinal dystrophies (IRDs) represent a heterogeneous group of disorders that primarily involve degeneration of the outer retina. These disorders occur in approximately 1 in 4000 individuals and affect 2 million patients worldwide.[10] To date, mutations in over 300 genes and loci have been identified to cause IRDs.[11] These disorders may occur sporadically or they can be familial; almost every mode of inheritance has been described.[10]

Both rod and cone photoreceptors can be affected in IRDs. In rod-specific disease, patients typically present with difficulties in dimly lit environments (nyctalopia) and they develop progressively narrowing peripheral visual fields. In cone-dominant disease, patients may present with impaired central vision, photo-aversion, and reduced color vision. In either case, visual function is significantly affected, and many patients develop legal blindness due to diminished visual fields or reduced visual acuity.

Both syndromic and non-syndromic forms of IRDs exist. A prototypical IRD is non-syndromic retinitis pigmentosa (RP). This disease is considered to be a rod-cone dystrophy, as rod photoreceptors are typically affected initially with subsequent degeneration of the cone photoreceptors. Patients present with nyctalopia and reduced peripheral vision. On fundoscopic examination, patients manifest the classic features of posterior subcapsular cataracts, vitreous cells, bone spicule intraretinal pigment migration, arteriolar attenuation, and optic disc pallor.[12] While there are currently no disease-modifying treatments available, ongoing clinical trials for RP exist that are evaluating the safety and efficacy of gene replacement therapy via subretinal

gene delivery using adeno-associated viral vectors. To date, clinical trials for *PDE6B, RS1, RLBP1, RPE65, CNGA3, CNGB3, CHM,* and *RPGR*-associated retinitis pigmentosa are underway, with results available from several of these trials.[10,13,14] Luxturna (voretigene neparvovec-rzyl) is a gene replacement therapy for *RPE65*-associated retinopathy that was approved by the FDA in 2017.[14]

Systemic manifestations accompany IRDs in approximately 20-30% of cases.[15] These syndromic IRDs can manifest with disease involving multiple organ systems including auditory, renal, cardiac, pulmonary, integumentary, and neurologic systems, among others. Patients with syndromic IRDs may first present to an ophthalmologist for evaluation. As a result, a careful examination for extraocular disease is essential and may facilitate more accurate clinical phenotyping and targeted genetic testing. In addition, earlier diagnosis of syndromic IRDs can enable subspecialty referral for surveillance for extraocular disease that might not have yet manifested.

3. Peroxisomal Biogenesis Disorders (PBDs)

Peroxisomal biogenesis disorders (PBDs), also known as Zellweger spectrum disorders (ZSDs), are a group of genetically and phenotypically heterogeneous conditions caused by aberrant peroxisome metabolism. Inherited in an autosomal recessive pattern, PBDs occur in 1 in 50,000 individuals and trigger a collection of disabilities including severe vision loss, sensorineural hearing loss, neurologic dysfunction (leukodystrophy and developmental delay), craniofacial abnormalities, vertebral anomalies, and liver dysfunction. Defects in 14 different *PEX* genes,

encoding peroxin proteins, involved in peroxisome membrane assembly, matrix protein import, and peroxisomal division, cause PBDs and lead to multisystem disease.[16] Specific laboratory investigations facilitate the diagnosis of a PBD. Elevated very-long chain fatty acids (VLCFAs), fatty acids containing 22 or more carbon atoms, may be detected in a patient's serum. In addition, elevated levels of pipecolic acid, pristanic acid, phytanic acid, and bile acid intermediates are typically present. Reduced levels of erythrocyte ether phospholipids (plasmalogens) may be seen in the serum as well.[17]

Mutations in *PEX1* and *PEX6* account for approximately 60% and 10% of all PBDs, respectively.[18] Although phenotypes can vary in severity, the PBDs may be considered a form of syndromic IRD where the majority of patients develop a generalized retinopathy. The PBDs represent four clinical syndromes that differ in disease onset and severity and include, from most to least severe: Zellweger syndrome, neonatal adrenoleukodystrophy, infantile Refsum disease, and Heimler syndrome. There are no specific clinical or laboratory distinctions between these syndromes; instead, they exist along a disease continuum.[18] There is a significant need to identify appropriate therapy, as there are no disease-modifying treatments currently available for PBDs. Only symptomatic therapies exist such as hearing aids, nutritional therapy, and vision aids.

3.1 Zellweger Syndrome (OMIM# 214100)

Zellweger syndrome (also known as cerebrohepatorenal syndrome) represents the most severe manifestation of the PBDs. Affected patients present in the early neonatal period with craniofacial malformations (high prominent forehead, hypoplastic supraorbital ridges, epicanthal

folds, midface hypoplasia, and large anterior fontanelle), hypotonia, seizures, psychomotor delay, neuronal migration defects and leukodystrophy, hepatomegaly, and renal cysts.[18] Ocular manifestations include corneal clouding, cataracts, glaucoma, and a generalized retinopathy with a severely diminished electroretinogram.[17] Zellweger syndrome is usually lethal within the first year of life. This severe phenotype is evident on the cellular level in cultured fibroblasts from patients with Zellweger syndrome. In these cells, there is a significantly reduced peroxisome abundance and the peroxisomal enzyme, catalase, is cytosolically distributed, suggesting impaired matrix protein import.[19]

3.2 Neonatal Adrenoleukodystrophy (NALD) (OMIM# 202370)

Patients with NALD manifest many of the same signs and symptoms as patients with Zellweger syndrome, albeit to a lesser degree of severity. A predominant differentiating feature includes the presence of a greater degree of central nervous system dysmyelination in NALD.[17] Consistent with a less severe phenotype than Zellweger syndrome, fibroblasts from patients with NALD have more peroxisomes than cells from patients with Zellweger syndrome (but still significantly fewer than control fibroblasts).[20]

3.3 Infantile Refsum Disease (OMIM# 266510)

Patients with infantile Refsum disease demonstrate milder manifestations of peroxisome dysfunction. These patients typically do not have congenital malformations but rather develop progressive disease beginning in early childhood. Initially, sensorineural hearing loss (SNHL)

and retinal dystrophy may be the most striking features. As a result, many patients are thought to have Usher syndrome.[21] There are several reports of patients with SNHL and IRD with negative results following testing using an Usher syndrome gene panel who are later discovered to have a peroxisomal disorder after additional research testing.[21,22] Peroxisomal genes are now starting to appear on commercial Usher syndrome panels (Retinal Dystrophy Panel, Blueprint Genetics, Helsinki, Finland). With time, we may find that peroxisomal disorders are more prevalent than once thought.

In addition to SNHL and IRD, patients with infantile Refsum disease can develop neurologic dysfunction, adrenal impairment, hepatic insufficiency, and renal oxalate crystals. Many patients present with some degree of developmental delay. Intellectual disability is variably present.[23] Similar to NALD, skin fibroblasts from patients with infantile Refsum disease have been shown to demonstrate a reduced number of peroxisomes, consistent with a peroxisomal biogenesis phenotype.[20]

3.4 Heimler Syndrome (OMIM # 234580)

Heimler syndrome represents the mildest PBD phenotype and was first described in 1991.[24] Similar to the other PBD groups, patients develop SNHL and IRD (although with a later onset); however, patients with Heimler syndrome also have the characteristic features of amelogenesis imperfecta and nail abnormalities.[25] Given that the latter two features may be subtle and require a conscientious clinical examination, patients with Heimler syndrome may also be confused as having Usher syndrome. Although not pathognomonic for Heimler syndrome, patients often

develop a maculopathy with cystic spaces present in the sub-foveal outer plexiform layer, evident clinically on optical coherence tomography (OCT).[26,27]

Hypomorphic variants in *PEX1, PEX6,* and *PEX26* have been reported to cause Heimler syndrome.[27] Skin fibroblasts from patients with Heimler syndrome have demonstrated a mosaic of protein import-competent and incompetent peroxisomes. This phenotype was found to be temperature sensitive where the majority of peroxisomes became import-incompetent when the cells were incubated at 40ºC, a finding evident in other peroxisomal disorders[25,28]

4. Peroxisome Biology

Peroxisomes are dynamic, single membrane-bound organelles that are present in nearly all eukaryotic cells. Composed of a lipid bilayer and a matrix lumen, peroxisomes vary in size (0.1 to 1μm in diameter) and number (100 to 1000 organelles per cell).[29,30] These organelles were originally described based on the presence of catalase and hydrogen peroxide-producing oxidases.[31] Currently, over 50 peroxisomal enzymes have been identified that facilitate diverse functions including β-oxidation of VLCFAs, α-oxidation of branched-chain fatty acids, bile acid and plasmalogen synthesis, and the detoxification of reactive oxygen species.[29] In addition, recent evidence even supports the role of peroxisomes in phagocytosis and the innate immune response.[32] Peroxisome interactions with endoplasmic reticulum (ER), lipid droplets, and mitochondria support the dynamic role these organelles play in lipid metabolism and other diverse cellular activities.[30] Peroxins and membrane-spanning peroxisomal membrane proteins (PMPs) orchestrate the many functions of this organelle.

4.1 Peroxisome Synthesis

Peroxisomes are dynamic organelles that can rapidly change their size and abundance in response to metabolic demand from internal or external cues. Peroxisomal biogenesis occurs via two separate mechanisms: *de novo* formation from the ER and fission of mature peroxisomes.

4.1.1 *De novo* Synthesis

De novo synthesis involves specialized regions of the ER that bud-off to become pre-peroxisomal vesicles. These vesicles are enriched in the PMPs Pex3 and Pex16.[33] In a process that is not fully understood, pre-peroxisomal vesicles fuse with other vesicles to acquire additional PMPs. Once the full repertoire of PMPs is acquired, the pre-peroxisomal vesicles import matrix proteins and complete the transition to a mature and functional peroxisome.[33]

4.1.2 Peroxisomal Fission

Mature peroxisomes are capable of undergoing organelle fission utilizing mechanisms similar to those in mitochondria. The first step of this process, elongation, occurs due to the oligomerization of the PMP Pex11 (β isoform). This oligomerization may be triggered by an environmental cue such as cell exposure to the omega-3 fatty acid docosahexaenoic acid (DHA).[34] Next, mitochondrial fission factor (Mff) recruits the dynamin-like protein-1 (Dlp1), a GTPase, to the membrane where it is activated, and the peroxisome membrane is pinched or

constricted in the second step. Finally, GTP hydrolysis provides the energy for peroxisomal fission mediated by Dlp1, and two daughter organelles are liberated.[34]

4.2 Peroxisomal Matrix Protein Import

Unlike mitochondria, peroxisomes do not contain their own genome. As a result, peroxisomes rely on a transport mechanism to import nuclear-encoded protein into the matrix to allow them to perform their diverse functions. Peroxisomes are unique in utilizing a post-translational protein transport system that is capable of importing fully folded and even oligomeric peptides.[30]

Peroxisomal matrix proteins are synthesized on free cytosolic ribosomes.[35] The majority of these proteins have a peroxisomal targeting signal (PTS) that destines the nascent polypeptide for the peroxisomal lumen. There are two types of PTS signals: PTS1 and PTS2. PTS1 is a C-terminal tripeptide, typically of the serine-lysine-leucine (SKL) sequence, that is recognized by the cytosolic shuttle Pex5. PTS2 is an N-terminal degenerate nonapeptide that is recognized by the shuttle Pex7. The majority of matrix proteins are imported via a PTS1-dependent pathway.[35]

Pex5, along with its PTS1-containing cargo, translocates to the peroxisomal membrane where the complex interacts with the docking/translocation module (DTM) that is composed of the transmembrane proteins Pex13 and Pex14 and the E3 ubiquitin ligases (Pex2, Pex10, and Pex12) (Figure 2). In a process that is not completely understood, a large membrane pore forms to facilitate entry of the protein cargo into the peroxisome.[36] At this time, Pex5 is membrane-bound at the DTM and needs to be released for subsequent rounds of matrix protein import. First, the

E3 ubiquitin ligases promote the monoubiquitination of Pex5 at a cysteine residue at position 11 in the primary sequence. Next, the receptor/exportomer module (REM), composed of Pex1, Pex6, and Pex26, extract Pex5 from the peroxisomal membrane in an ATP-dependent process. Pex5 is released from the peroxisomal membrane into the cytosol where it can interact with other PTS1-containing proteins. The mechanism for import of PTS2-containing proteins is similar except it involves the cytosolic shuttle Pex7 in conjunction with Pex5 (long isoform).[35]

Pex1 and Pex6 belong to a group of ATPases called the AAA ATPases (*A*TPases *A*ssociated with diverse cellular *A*ctivities). These proteins form heterohexameric units that are anchored to the peroxisomal membrane through interactions with Pex26. Interestingly, these proteins belong to the only step of peroxisomal protein import that requires ATP.[36] Despite Pex1 and Pex6 having established roles in matrix protein import, the precise means by which these proteins extract monoubiquitinated Pex5 from the peroxisomal membrane is currently unknown. Furthermore, it is unknown whether the REM interacts with proteins other than Pex5.[36] Recently, it has been demonstrated that AAA ATPases, specifically Pex1 and Pex26, play a role in protecting the peroxisome from degradation.[37]

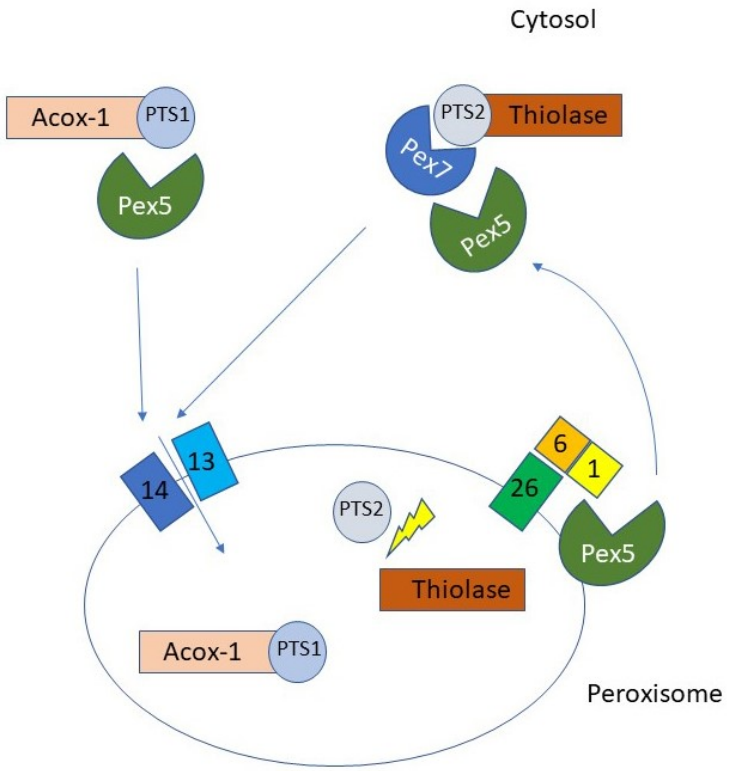

Figure 2. A model of peroxisomal matrix protein import. Nascent polypeptides synthesized in the cytosol that are destined for the peroxisomal lumen are labelled with either a C-terminal PTS1 tripeptide or an N-terminal PTS2 nonapeptide. Pex5, a cytosolic shuttle, delivers PTS1-containing cargo to the docking/translocation module (DTM) composed of Pex13 and Pex14. Cargo containing the PTS2 nonapeptide is delivered to the DTM by a separate cytosolic shuttle, Pex7, in conjunction with Pex5 (long isoform). A membrane pore forms, and the protein cargo is delivered inside the peroxisome. Once in the lumen, the PTS2, but not the PTS1, targeting signal is cleaved off. Pex5 is removed from the peroxisomal membrane by the action of the receptor/exportomer module (REM) composed of Pex1, Pex6, and Pex26. Pex1 and Pex6 utilize ATP to extract Pex5 from the peroxisomal membrane so that it is available for subsequent rounds of matrix protein import.

4.3 Lipid Metabolism

Both peroxisomes and mitochondria are capable of metabolizing fatty acyl-CoAs via β-oxidation.[38] The overall process of β-oxidation in both organelles is similar. First, a dehydrogenation reaction produces a *trans* double bond between the two carbons adjacent to the carboxy terminus. Next, a hydration reaction and a second dehydrogenation step generate a 3-ketoacyl-CoA molecule. Finally, thiolytic cleavage with the enzyme thiolase occurs and liberates an acetyl-CoA group. This series of reactions repeats with each cycle shortening the fatty acyl-CoA chain by two carbons.[38]

Although similarities exist in lipid processing in peroxisomes and mitochondria, peroxisomes are distinct in that they are where β-oxidation of VLCFAs preferentially occurs.[39] As a result, elevated levels of VLCFAs in a patient's serum suggest peroxisomal dysfunction.[11] In addition, peroxisomes are capable of metabolizing branched-chain fatty acyl-CoAs through a process known as α-oxidation. Phytanic acid, a branched-chain fatty acid, undergoes α-oxidation in peroxisomes where a terminal carboxyl group is removed, facilitating subsequent β-oxidation reactions in peroxisomes or mitochondria.[38] Patients with PBDs have increased levels of serum phytanic acid which result in the decoupling of oxidative phosphorylation in mitochondria, enhanced reactive oxygen species generation, and perturbed cellular calcium signaling, ultimately leading to cell death.[40] Therefore, patients should be counseled to avoid foods with high phytanic acid content, such as fish, and foods derived from ruminant animals.[41]

5. Peroxisomes and the Retina

Despite peroxisomes being ubiquitous organelles, they are dynamic structures that can differ in number, size, and enzymatic composition in various tissues and organs.[29] While retinal dystrophy is a common ocular phenotype in many PBDs, the precise mechanisms by which aberrant peroxisomal metabolism leads to retinopathy is relatively unstudied.

Peroxisomes have been identified in all layers of the retina, including the RPE.[42-46] Deguchi and colleagues have suggested that peroxisomes facilitate the metabolism of rod and cone outer segment membranes in the RPE since these photoreceptor membranes contain an abundance of DHA, a VLCFA.[47] In fact, peroxisomes have recently been demonstrated to interact with phagosomes in the RPE containing disc outer segments before the phagosomes fuse with lysosomes.[48] These findings suggest a role for peroxisomes in photoreceptor membrane recycling.[49] Finally, other studies suggest that peroxisomes play an important role in protecting the RPE, a highly metabolically active cell, from oxidative stress.[44,46,50]

While studies have speculated on the roles of peroxisomes in various regions of the retina, the localization and expression of individual peroxins and peroxisomal membrane proteins are important since these are the proteins implicated in disease. Pex6 has been identified throughout the human retina and it is particularly enriched at the junction between photoreceptor inner and outer segments, just distal to the connecting cilium.[44] Precisely how mutations in *PEX6* lead to retinopathy is not well established; however, the enrichment of Pex6 at the level of the photoreceptors supports its importance in the outer retina.[44]

6. Clinical Case

This research study originated from observations made on a patient with retinal degeneration who presented to an ocular genetics clinic. He was a 12-year old child of French-Canadian/Swedish/Welsh origin who had severe congenital SNHL and retinopathy leading to significant nyctalopia and vision loss. We later discovered that his first-cousin had been clinically diagnosed with Zellweger syndrome and had died at 18 months of age (Figure 3). Our patient's past medical history was otherwise unremarkable.

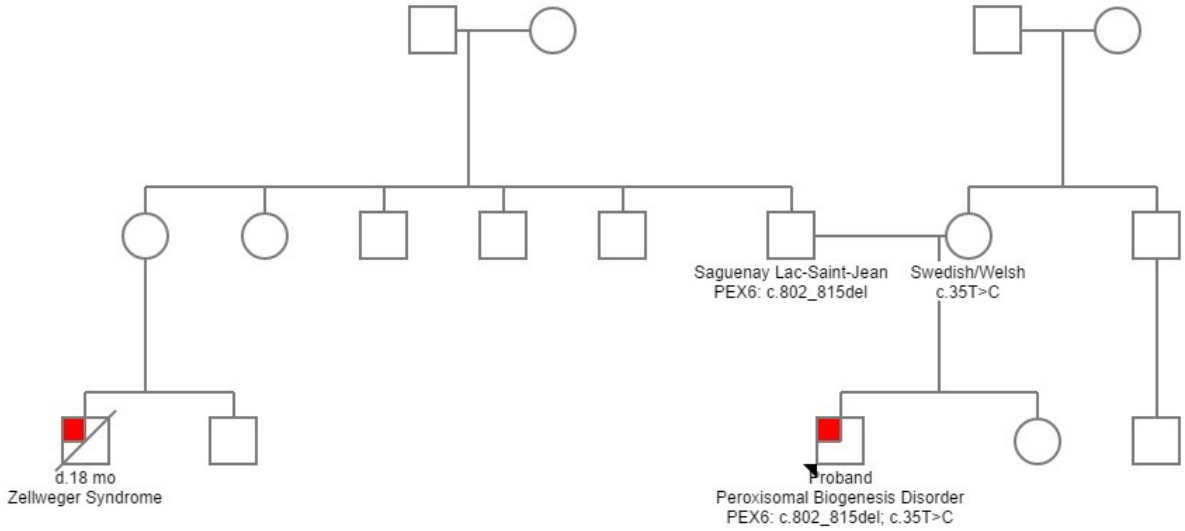

Figure 3. Three-generation pedigree of a family with a peroxisomal biogenesis disorder (red box). The proband, indicated with an asterisk, carries compound heterozygous mutations in *PEX6*: c.802_815del GACGCACTGGCGCT and c.35T>C (p.Phe12Ser). The proband's first cousin, who was not genotyped, passed away from Zellweger syndrome at 18 months of age.

On ocular examination, his visual acuity was 20/150 OD and 20/150 OS. His intraocular pressures were normal. His extraocular movements were full and there was no strabismus. His pupils were equal and reactive to light and accommodation. Anterior segment examination was unremarkable but posterior segment examination revealed a mottled fundus appearance with granular RPE changes OU (Figures 4A and 4B). The optic nerves appeared grossly normal; however, the maculae demonstrated prominent cystic cavities on optical coherence tomography (OCT) imaging (Figures 4C and 4D). Given concern for an underlying retinal dystrophy, a full field electroretinogram (ffERG) was ordered. The ffERG measures electrical signals generated by the retina when the eye is in a dark- or light-adapted state. This test demonstrated significantly reduced rod- and cone-driven responses, confirming an underlying retinopathy. Given the co-occurrence of congenital SNHL and retinal dystrophy, a diagnosis of Usher syndrome was postulated. Usher syndrome is the most common cause of inherited combined deafness and blindness.[51] Subsequently, an Usher syndrome gene panel, consisting of 15 genes, was ordered to molecularly characterize the phenotype (Blueprint Genetics, Helsinki, Finland). Results of this gene panel were negative; however, the lab reflexively tested for genes associated with peroxisomal disorders as these conditions have recently been identified in other patients with a clinical diagnosis of Usher syndrome but non-revealing genetic testing.[21] Compound heterozygous mutations in *PEX6* were discovered: c.802_815del GACGCACTGGCGCT and c.35T>C (p.Phe12Ser). Both variants segregated with disease with the deletion inherited paternally and the missense mutation inherited maternally. The paternally inherited deletion has been demonstrated to exhibit a founder effect in a Saguenay-Lac-St-Jean French-Canadian population and is present in patients diagnosed with Zellweger syndrome.[52] The missense variant has also been previously reported in a patient with a peroxisomal biogenesis disorder.[53]

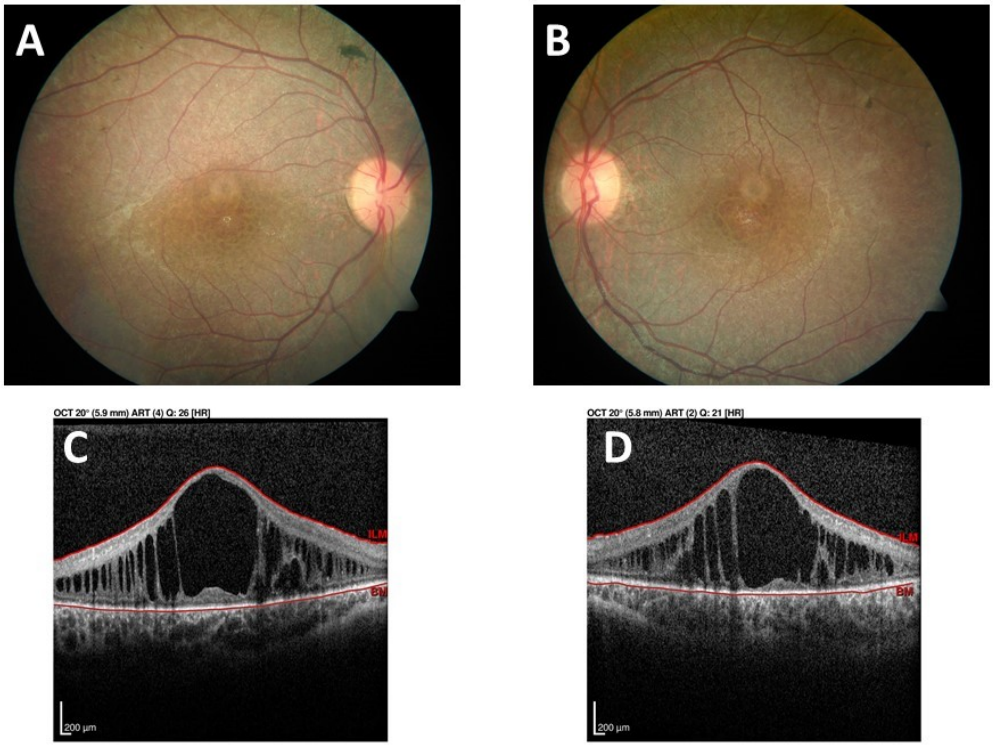

Figure 4. Color fundus photographs of the posterior poles of the right (A) and left (B) eyes in a 12-year-old patient with a peroxisomal biogenesis disorder. Both fundi demonstrate a mottled appearance to the RPE with trace intraretinal pigment migration. The optic nerves appear normal but there is mild retinal arteriolar attenuation in both eyes. Optical coherence tomography (OCT) B-scan images at the level of the fovea in the right (C) and left (D) eyes. There are large cystoid cavities that significantly distort the retinal architecture in both eyes.

Biochemical analysis of the patient's serum revealed mildly elevated very-long chain fatty acids: C26:0/C22:0 0.028µmol/L (normal <0.020) and C24:0/C22:0 1.05µmol/L (normal 0.44-1.16). Pristanic acid, phytanic acid, and pipecolic acid levels were all within normal limits. A brain MRI demonstrated diffuse white matter changes in the thalami, brainstem, cerebellum, and periventricular regions, consistent with a peroxisomal disorder. Given the above findings, the patient was diagnosed with a peroxisomal biogenesis disorder due to biallelic mutations in *PEX6.* In addition to regular ophthalmology follow-up, the patient was referred to medical genetics for further systemic evaluation and dietary intervention.

7. Hypothesis and Study Importance

Given the rare occurrence of PBDs and that a significant portion of PBDs is diagnosed in patients with severe phenotypes that result in death at an early age, our patient's milder presentation provided a unique opportunity to study the mechanism of disease both clinically over time and at a cellular level. Our lab sought to understand how our patient's specific mutations in a peroxisomal gene, *PEX6*, led to impaired cell metabolism. Evaluating our patient's specific disease factors aligns with a personalized approach to health delivery (Precision Medicine) and facilitates a deeper understanding of peroxisomal function. Genetic disorders will likely benefit most from targeted genetic therapies; these treatments depend on a thorough understanding of disease mechanisms in patients.

A recent study suggested that one of the primary roles of members of the AAA ATPase protein family, Pex1, Pex6, and Pex26, was to protect the peroxisome from degradation, a process

known as pexophagy.[37] The authors demonstrated that HeLa cells transfected with *PEX1* or *PEX26* siRNA led to significantly reduced peroxisome abundance. In a series of experiments, the authors concluded that the primary defect was one of excessive peroxisomal degradation (pexophagy) as opposed to reduced matrix protein import. Furthermore, the authors demonstrated that treating cells with chloroquine, a drug used therapeutically in several autoimmune disorders, inhibited pexophagy and restored peroxisome abundance. Chloroquine acts as an inhibitor of cell autophagy by elevating the pH within lysosomes.[37]

Given that *PEX6* was not evaluated in their study, we hypothesized that mutations in *PEX6*, the other member of the AAA ATPase family that forms a complex with Pex1 and Pex26, would also lead to reduced peroxisome abundance as a result of increased pexophagy. We sought to test this hypothesis *in vitro* by studying the peroxisomes in patient-derived skin fibroblasts.

MATERIALS AND METHODS

8.1 Cell Culture

Human embryonic kidney 293T (HEK293T) cells (Thermo Scientific, Cat. No. HLC4517, Waltham, MA) were grown in Cytiva HyClone Dulbecco's Modified Eagle Medium (DMEM) (Thermo Scientific, Cat. No. SH30243LS, Waltham, MA) with L-glutamine, sodium pyruvate, and 10% Gibco Fetal Bovine Serum (FBS) (Thermo Scientific, Cat. No. 12483-020, Canada) with penicillin 50 IU/mL and streptomycin 50 µg/mL added. Skin fibroblasts were collected from the patient and from each of his parents by performing a 3 to 4mm superficial dermal biopsy on the underside of the upper arm. A local anesthetic consisting of 1% lidocaine with 1 in 100,000 epinephrine was used for the procedure. Our lab had available a skin fibroblast cell line that was used as a control and was wild-type for *PEX6*. Skin fibroblasts were cultured in the same medium conditions except 15% FBS was used. Cells were incubated at 37°C-and at 5% CO_2 concentration.

8.2 Antibodies

Antibodies were purchased and used for western blot and immunofluorescence assays as indicated in Table 1.

Table 1. A list of antibodies used in western blot and immunofluorescence assays

Antibody	Clonality and Source	Manufacturer and Catalogue Number	Application and Dilution
β-actin	Monoclonal mouse	Santa Cruz (sc-69879)	WB: 1:500
β-actin	Polyclonal rabbit	Abcam (ab8227)	WB: 1:2000
FLAG	Monoclonal mouse	MilliporeSigma (F1804)	WB: 1:1000
Pex1	Polyclonal rabbit	Abcam (ab217059)	WB: 1:1000
Pex5	Polyclonal rabbit	Abcam (ab204444)	WB: 1:1000
Pex6	Monoclonal mouse	Santa Cruz (sc-271813)	WB: 1:100
Pex14	Polyclonal rabbit	Proteintech (10594-1-AP)	WB: 1:1000 IF: 1:100
Pex14	Polyclonal mouse	MilliporeSigma (SAB1409439)	WB: 1:1000 IF: 1:100
Pex26	Polyclonal rabbit	Abcam (ab235084)	WB: 1:1000
Pmp70/ABCD3	Polyclonal rabbit	Abcam (ab3421)	WB: 1:1000
Thiolase/ACAA1	Polyclonal rabbit	Abcam (ab154091)	WB: 1:1000 IF: 1:100

WB = western blot; IF = immunofluorescence

8.3 Cell Harvesting

HEK293T cells and skin fibroblasts were grown to confluency on 6-well plates. The growth medium was removed, and the cells were washed three times with 1mL of Cytiva HyClone Phosphate Buffered Saline (PBS) (Thermo Scientific, Cat. No. SH3025602, Waltham, MA). Cell lysis was performed with 100 µL of ice-cold RIPA buffer (Boston BioProducts, Cat. No. BP-407, Ashland, MA) with protease inhibitor (Thermo Scientific, Cat. No. 78415, Waltham, MA) added to each well. The cells were mechanically harvested using cell scrapers (Falcon, Cat. No. CA15621-005, Franklin Lakes, NJ). The cell lysates were incubated on ice for 15 minutes. Next, the lysates were centrifuged at 16,100 g for 15 minutes at 4ºC (Eppendorf, Cat. No. 2262140-8, Standard Rotor FA-45-24-11, Westbury, NY), and the supernatant was collected. Protein concentration was determined via a colorimetric technique using the Pierce BCA Protein Assay Kit (Thermo Scientific, Cat. No. 23225, Waltham, MA).

8.4 SDS-PAGE and Western Blotting

Pre-cast 12% Mini PROTEAN TGX SDS-PAGE gels (Bio-Rad, Cat. No. 4561044, Hercules, CA) were used and 30 µg of protein were loaded in each lane. Two µL of Chameleon Duo Pre-Stained Protein Ladder (LI-COR, Cat. No. 928-60000, Lincoln, NE) were used as a protein size standard in a single lane. The gels were run at room temperature in a Mini PROTEAN Tetra Electrode Assembly/Running Cartridge (Bio-Rad, Cat. No. 1658037, Hercules, CA) using approximately 1 L of running buffer (25 mM Tris, 190 mM glycine, 0.1% SDS) for 80 minutes at 110 V. The separated proteins from the gel were then transferred onto nitrocellulose

membrane (0.45 μm pore size) using the Mini Trans-Blot Central Core and Buffer Tank (Bio-Rad, Cat. No. 1703930, Hercules, CA) using approximately 1 L of transfer buffer (25 mM Tris, 190 mM glycine, 20% methanol) for 60 minutes at 100 V at 4ºC.

The membrane was then retrieved and Intercept PBS Blocking Buffer (LI-COR, Cat. No. 927-70001, Lincoln, NE) was applied. The blot was agitated for 1 hour at room temperature on a tabletop shaker. Next, the blocking buffer was removed, primary antibodies (in the dilutions given in Table 1) were added to the membrane, and the blot was left overnight to incubate at 4ºC on a tabletop shaker. On the following morning, the primary antibodies were removed, and the membrane was washed for 5 minutes with PBS-T (PBS with 0.05% Tween-20). This was repeated three times. Next, goat-anti mouse (Alexa Fluor 680) and goat-anti rabbit (Alexa Fluor 800) secondary antibodies (LI-COR, Lincoln, NE) were added, and the membrane was placed on the shaker for 45 minutes at room temperature. Then, the membrane was washed twice, 10 minutes each time, with PBS and then once for 10 minutes with PBS-T. The blots were then scanned using the Odyssey CLx imaging system (LI-COR, Lincoln, NE).

8.5 Immunofluorescence Microscopy

HEK293T cells and skin fibroblasts were plated on #2 glass coverslips (22 mm x 22 mm) (Fisher Scientific, Cat. No. 12-540B, Waltham, MA) and grown to approximately 50% confluency. The growth medium was removed, and cells were washed twice with 1 mL of PBS-T. Next, 1 mL of 2% paraformaldehyde was added to each well and the cells were incubated for 20 minutes at room temperature. Then, the paraformaldehyde was removed, and the cells were washed twice

with 1 mL of PBS-T. Following this, 1mL of blocking solution was added (1% bovine serum albumin (BSA) and 0.5% Triton X-100 in PBS) for 15 minutes at room temperature. Primary antibodies (in the dilutions given in Table 1) were then added to each coverslip in 100 µL of blocking solution for 1 hour at room temperature. The cells were then washed twice with 1 mL of PBS-T. Next, donkey-anti rabbit (Alexa Fluor 555) (Invitrogen, Cat. No. A31572, Carlsbad, CA) and goat-anti mouse (Alexa Fluor 488) (Invitrogen, Cat. No. A10680, Carlsbad, CA) secondary antibodies were added, and the cells were incubated for 1 hour at room temperature. After two further washes with 1 mL of PBS-T, DAPI was added (0.2 µL of 5 mg/mL solution in 100 µL PBS) for 5 minutes. An additional two washes with 1 mL of PBS-T were performed, and the coverslips were mounted onto glass microscope slides using ProLong Glass Antifade Mountant (Invitrogen, Cat. No. P36984, Carlsbad, CA). The slides were allowed to dry overnight in the dark and were then stored, protected from light, at 4ºC. Immunofluorescence images were captured with a spinning disc confocal microscope (Quorum Technologies, Puslinch, ON) at the Cell Imaging Center at the University of Alberta. Multiple cells (> 20 cells) from each slide were examined and images were captured of representative samples.

8.6 Plasmid Preparation and Subcloning

We purchased a *PEX6* pcDNA3.1+/C-(K)-DYK expression plasmid (GenScript, Clone ID OHu26056D, Piscataway, NJ) and transformed DH5α competent *E. coli* cells (Thermo Scientific, Cat. No. 18265017, Waltham, MA). To create a *PEX6* c.35T>C expression plasmid, we utilized a forward primer (5′-GATCGGATCCTTATGGCGGTCGCTGTCTTGCGGGTCCTGGAGCCCTCTCCGACCGAG

-3′) that included the *PEX6* c.35T>C point mutation and a BamHI restriction site. In addition, we utilized a reverse primer (5′-GATCGCGGCCGCCTAGCAGGCAGCAAACTTGCGC-3′) that included a NotI restriction site. We amplified the *PEX6* cDNA fragment by PCR and incorporated the point mutation within the forward primer. We then performed a restriction digestion reaction with FastDigest BamHI (Thermo Scientific, Cat. No. FD0054, Waltham, MA) and FastDigest NotI (Thermo Scientific, Cat. No. FD0594, Waltham, MA) of the plasmid and PCR product and then performed a ligation reaction to generate the *PEX6* c.35T>C pcDNA3.1+/C-(K)-DYK expression plasmid. The plasmid and insert were confirmed by a combination of restriction digestion and Sanger sequencing.

We purchased the PTS1 expression plasmid pEGFP-C1+SKL (Addgene, Cat. No. 53450, Watertown, MA) for the *in vivo* PTS1-mediated protein import assay. The *in vivo* green fluorescent protein signal was assessed with the EVOS M5000 Imaging System (Thermo Scientific, Cat, No. AMF5000, Waltham, MA).

We also purchased a *PEX5* pCMV6 Myc- and DDK-tagged expression plasmid (OriGene, Cat. No. RC226051, Rockville, MD) and transformed DH5α competent *E. coli* cells (Thermo Scientific, Cat. No. 18265017, Waltham, MA).

8.7 CRISPR/Cas9-mediated *PEX6* Deletion

We utilized the Alt-R CRISPR-Cas9 system (IDT, Newark, NJ) with a predesigned guide RNA (crRNA) (5′-/AltR1/ACC GCA AAG GAG GAC ACC ACG UUU UAG AGC UAU

GCU/AltR2/-3′) and fluorescently labelled trans-activating crRNA ATTO 550 (tracrRNA) to generate *PEX6* knock-out HEK293T cells. Briefly, we combined the crRNA and tracrRNA to generate an RNA duplex. The ribonucleoprotein (RNP) complex was created by adding the Cas9 nuclease, and this complex was transfected into 400,000 HEK293T cells per well in a 12-well plate using Lipofectamine CRISPRMAX Cas9 Transfection Reagent (Thermo Scientific, Cat. No. CMAX0001, Waltham, MA) in Opti-MEM Reduced Serum Medium (Thermo Scientific, Cat. No. 31985062, Waltham, MA). The cells were incubated for 48 hours at 37ºC.

Fluorescently labelled transfected cells were sorted using fluorescence-activated cell sorting (FACS) and seeded as individual cells into each well of a 96-well plate. These cells were allowed to expand over 2 weeks. To determine the editing efficiency, the Alt-R Genome Editing Detection Kit (IDT, Newark, NJ) with T7EI enzyme was used. Following PCR amplification of the *PEX6* CRISPR site, Sanger sequencing was performed, and we identified a homozygous single base deletion in exon 1 of *PEX6* (c.544delG) in one of the colonies. Quantitative PCR was performed to confirm minimal *PEX6* gene expression. The *PEX6* c.544delG HEK293T cells were selected for downstream assays and are referred to as *PEX6* knock-out HEK293T cells for the remainder of this study.

8.8 Transfection

HEK293T cells were seeded at 250,000 cells per well in a 6-well plate 18-24 hours before transfection so that cells were 60-80% confluent. Next, 10 µL of Lipofectamine 2000 reagent (Thermo Scientific, Cat. No. 11668019, Waltham, MA) were diluted into a total of 150 µL of

Opti-MEM Reduced Serum Medium (Thermo Scientific, Cat. No. 31985062, Waltham, MA), and 4 μg of plasmid was diluted into a total of 150 μL of Opti-MEM medium. The two mixtures were combined and incubated for 5 minutes at room temperature. Next, 250 μL of the plasmid-lipid complex were added dropwise to each well. The cells were incubated at 37ºC and 5% CO_2 concentration, and they were processed 72 hours later.

Skin fibroblasts from the patient, from each of his parents, and a control sample were transfected using the Human Dermal Fibroblast Nucleofector Kit (Lonza, Cat. No. VPD-1001, Hayward, CA). A T75 flask containing confluent fibroblasts was trypsinized, and 500,000 cells were pipetted into a 1.5 mL Eppendorf tube and centrifuged for 5 minutes at 400 g (Eppendorf, Cat. No. 2262140-8, Standard Rotor FA-45-24-11, Westbury, NY), and the cell pellet was retained. Next, 2 μg of plasmid was combined with 110 μL of the Nucleofector Solution (containing Supplement 1), and the resulting solution was used to resuspend the cell pellet. This solution was placed into an aluminum cuvette and then into the Nucleofector 2b device (Lonza, Hayward, CA). Following electroporation, the solution was transferred into a single well containing growth medium in a 6-well plate. The fibroblasts were incubated at 37ºC and 5% CO_2 concentration and the *in vivo* PTS1 expression plasmid GFP signal was examined 48 hours later.

8.9 Image Processing and Statistics

Microscopy images were processed using ImageJ software (NIH, Bethesda, MD). Images were enhanced in Photoshop (Adobe, San Jose, CA) using the levels feature without reaching saturation. Western blot data were quantified using Image Studio Lite software (version 5.2), and

the results were compared by using Student's t-test with $\alpha = 0.05$ considered as statistically significant. Statistical analysis was performed in Microsoft Excel 2016 (Microsoft, Redmond, WA). Figures were created using Microsoft PowerPoint 2016 (Microsoft, Redmond, WA).

RESULTS

9.1 Patient-specific *PEX6* mutations lead to reduced Pex6 protein levels

To determine the effect of the patient-specific mutations in *PEX6*, c.802_815del and c.35T>C, on the abundance of Pex6 protein, endogenous Pex6 protein levels in each fibroblast line were determined by western blot. Pex6 protein was significantly reduced in patient fibroblasts (*PEX6* c.802_815del/c.35T>C) to 14% of control (WT/WT) levels ($P = 0.0001$; n = 3) (Figure 5). Pex6 abundance in the father's (*PEX6* WT/c.802_815del) and mother's (*PEX6* WT/c.35T>C) fibroblasts did not differ from one other but was significantly reduced to approximately 60% of control fibroblast Pex6 levels ($P = 0.01$; n = 3) (Figure 5).

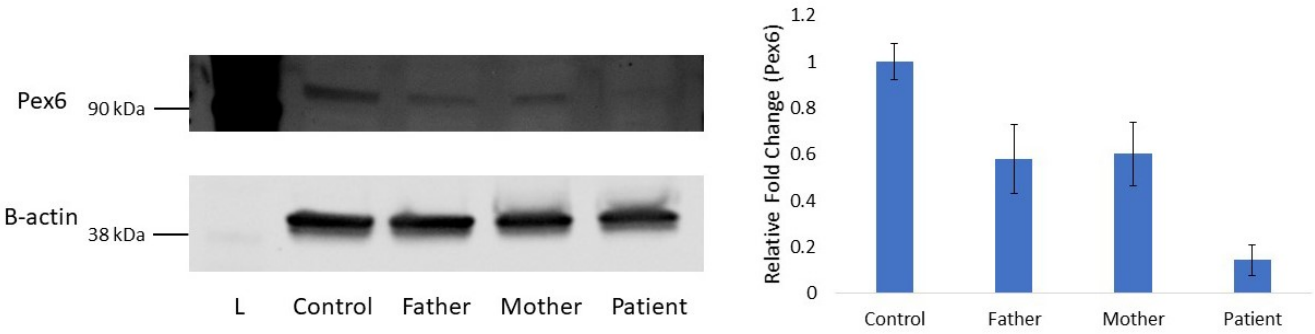

Figure 5. Endogenous amounts of Pex6 protein in skin fibroblast lysates. Pex6 was significantly reduced in the father's fibroblasts ($P = 0.01$), mother's fibroblasts ($P = 0.01$) and patient's fibroblasts ($P = 0.0001$) compared to control fibroblasts (n = 3 experimental replicates). L = ladder (protein size standard).

9.2 Mutations in *PEX6* do not result in reduced peroxisome abundance

Given the prior evidence of reduced peroxisome abundance in cells devoid of Pex1 or Pex26,[37] we evaluated peroxisome abundance in fibroblasts harboring mutations in *PEX6* (the third member of the receptor exportomer module). To determine the effect of patient-specific mutations in *PEX6* on peroxisome abundance, Pex14, a peroxisomal membrane protein, was used as a surrogate marker for peroxisome abundance on a western blot.[54] There was no significant difference in Pex14 protein levels between the father's, mother's, and patient's fibroblasts compared to control fibroblasts ($P = 0.64$; n = 3) (Figure 6).

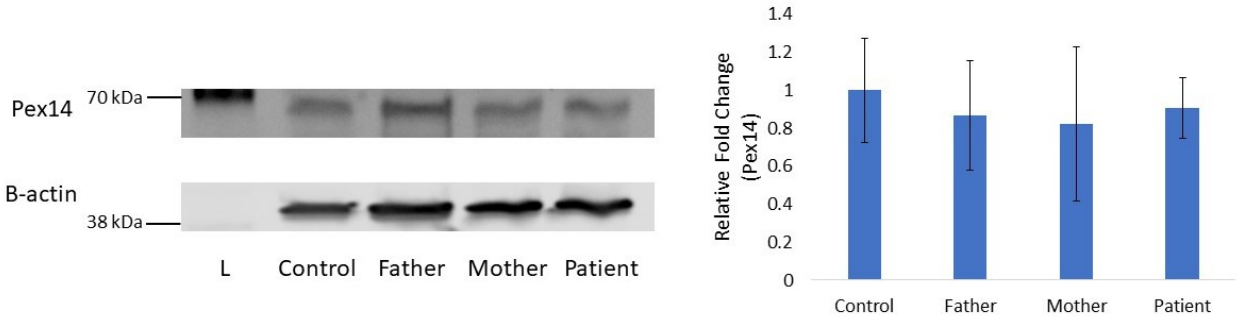

Figure 6. Endogenous amounts of Pex14 protein in skin fibroblast lysates. Pex14, a peroxisomal membrane protein and surrogate marker for peroxisome abundance, did not differ significantly between the father's, mother's, and patient's fibroblasts compared to control fibroblasts (control vs patient fibroblasts: $P = 0.64$; n = 3 experimental replicates). L = ladder (protein size standard).

9.3 Characterizing a CRISPR/Cas9-derived *PEX6* knock-out cell line

Given that the fibroblasts with compound heterozygous *PEX6* mutations arose from a patient with a peroxisomal biogenesis disorder on the milder end of the spectrum, we decided to generate a *PEX6* knock-out line in HEK293T cells to emulate a more severe peroxisomal phenotype. A CRISPR/Cas9 system generated a homozygous *PEX6* c.544delG in exon 1 in HEK293T cells. This single nucleotide deletion would be expected to lead to nonsense-mediated mRNA decay. On western blot, endogenous Pex6 protein was essentially absent in the *PEX6* knock-out cells compared to wild-type HEK293T cells (Figure 7).

To evaluate the effect of an absence of Pex6 on the other two members of the receptor exportomer module, Pex1 and Pex26 were probed on western blot in the wild-type and *PEX6* knock-out cells. Pex1 protein did not differ significantly in quantity in *PEX6* knock-out cells compared to control cells ($P = 0.24$; n = 3). However, Pex26, a single-pass peroxisomal membrane protein that anchors the Pex1:Pex6 heterohexamer to the peroxisome, was significantly reduced in *PEX6* knock-out cells by 60% compared to wild-type cells ($P = 0.006$; n = 3) (Figure 8).

To determine whether peroxisome abundance is influenced by an absence of Pex6, endogenous levels of Pex14, a surrogate marker of peroxisome abundance, was evaluated on a western blot. Unlike in patient fibroblasts with compound heterozygous mutations in PEX6, Pex14 was significantly reduced in *PEX6* knock-out cells by 41% compared to wild-type HEK293T cells ($P = 0.04$; n = 3) (Figure 9).

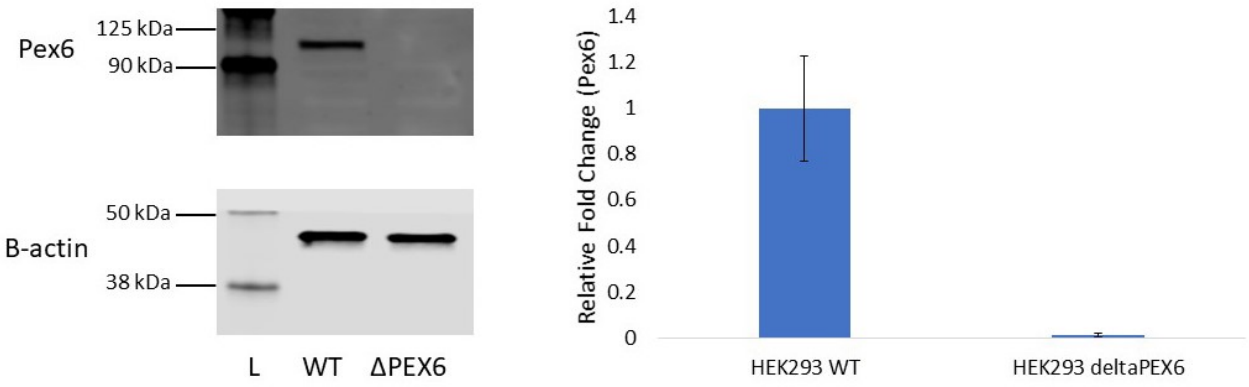

Figure 7. Endogenous amounts of Pex6 protein in HEK293T wild-type cell lysates and *PEX6* knock-out cell lysates. Pex6 protein is essentially absent in the *PEX6* knock-out cell lysates compared to wild-type cells ($P = 0.002$; n = 3 experimental replicates). L = ladder (protein size standard).

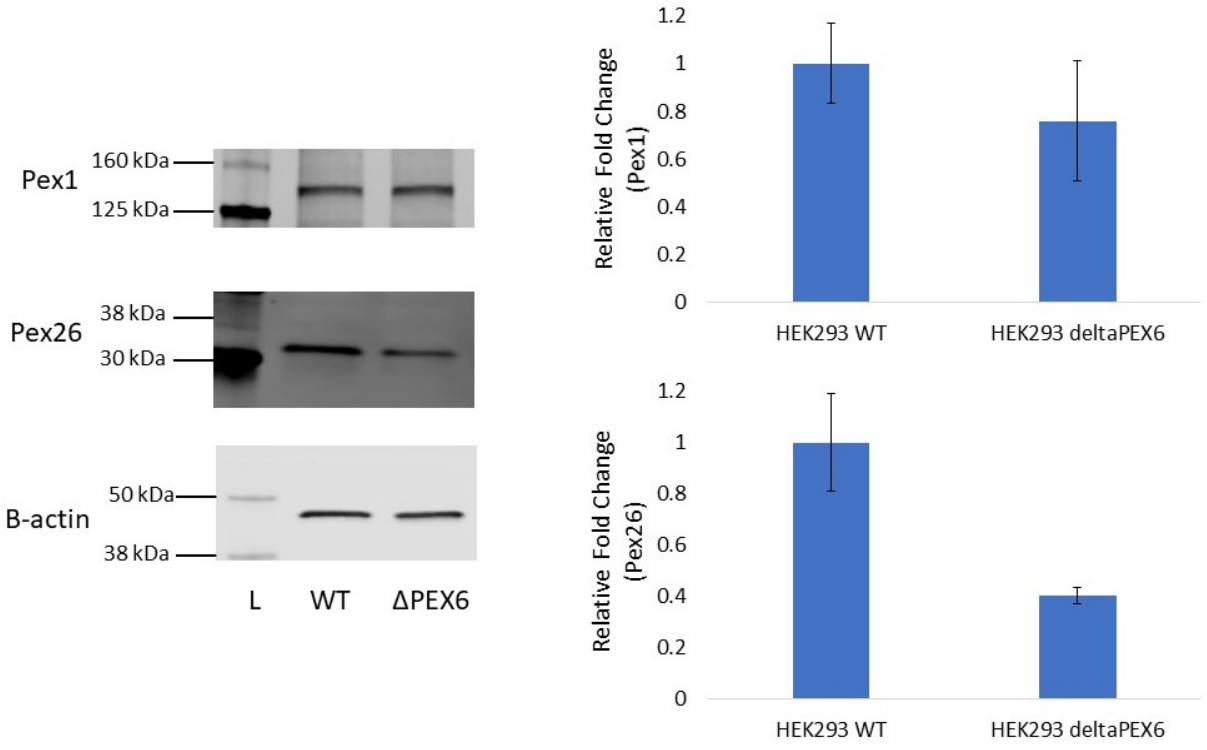

Figure 8. Endogenous amounts of Pex1 and Pex26 in HEK293T wild-type cell lysates and *PEX6* knock-out cell lysates. The Pex1 protein quantity did not differ significantly in *PEX6* knock-out cells compared to control cells ($P = 0.24$; n = 3). Pex26 protein was significantly reduced in *PEX6* knock-out cells by approximately 60% compared to wild-type cells ($P = 0.006$; n = 3 experimental replicates). L = ladder (protein size standard).

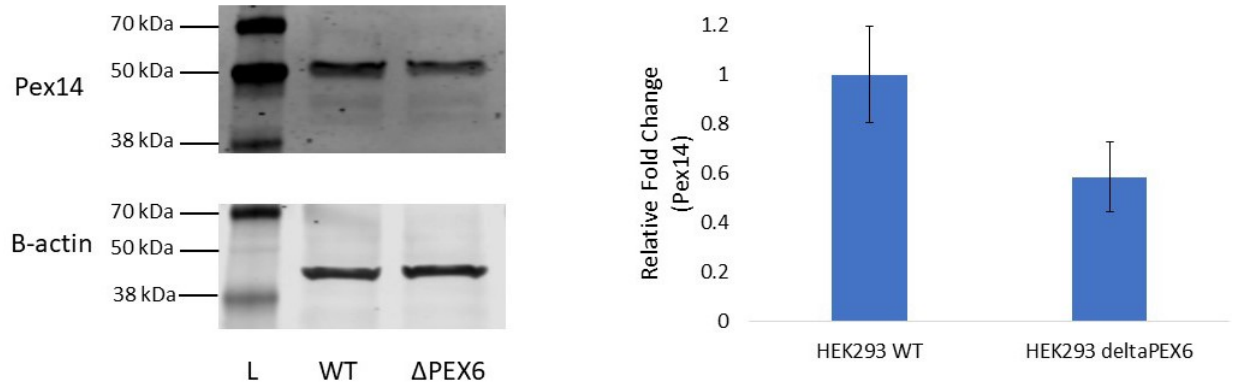

Figure 9. Endogenous amounts of Pex14 protein in HEK293T wild-type cell lysates and *PEX6* knock-out cell lysates. Pex14 protein was significantly reduced in *PEX6* knock-out cells by approximately 40% compared to wild-type cells ($P = 0.04$; n = 3 experimental replicates).

9.4 PTS1-mediated peroxisomal matrix protein import is disrupted in patient fibroblasts and *PEX6* knock-out cells

We were unable to detect a difference in peroxisome abundance on western blot between control fibroblasts and patient fibroblasts using both Pex14 (Figure 6) and Pmp70, a separate peroxisomal membrane protein (Supplementary Figure 1), as surrogate markers of peroxisome abundance. Given this result, our hypothesis that mutations in *PEX6* would lead to reduced peroxisome abundance and excess organelle degradation (pexophagy), similar to previously published *PEX1* and *PEX26* siRNA experiments,[37] was not supported. As a result, we decided to interrogate matrix protein import, one of the major roles of Pex6, to evaluate whether this process was disrupted instead in our patient's cells (Figure 2).

Transfecting by electroporation, a GFP-PTS1 expression plasmid was introduced into control fibroblasts and patient fibroblasts. After 48 hours, the distribution and intensity of GFP signal was evaluated using an EVOS cell imaging system. PTS1 is a tripeptide containing a serine-lysine-leucine (SKL) sequence that is present on the C-terminus of nascent polypeptides synthesized in the ER and targets proteins to the peroxisome. Control fibroblasts demonstrated an intracellular punctate GFP signal, as would be expected if the GFP-PTS1 was successfully localized to the peroxisomes. The patient fibroblasts, however, demonstrated a diffuse cytosolic GFP signal with very few puncta evident, suggesting impaired PTS1-mediated peroxisomal protein import (Figure 10). Analysis of GFP-PTS1 distribution in the father's and mother's fibroblasts revealed a similar pattern to control fibroblasts (data not shown).

To evaluate the PTS1 protein import pathway *in vivo* in the CRISPR/Cas9-mediated *PEX6* knock-out HEK293T cells, the same GFP-PTS1 expression plasmid was transfected into control and *PEX6* knock-out cells using a lipofectamine reagent. Similar to control fibroblasts, wild-type HEK293T cells demonstrated intracellular punctate GFP signal, suggesting appropriate PTS1-mediated targeting of proteins to peroxisomes. The *PEX6* knock-out cells, however, demonstrated diffuse cytosolic GFP signal with no appreciable puncta, similar to the patient fibroblasts (Figure 10). In both cases, defects in *PEX6* appeared to cause impaired PTS1-mediated peroxisomal protein import.

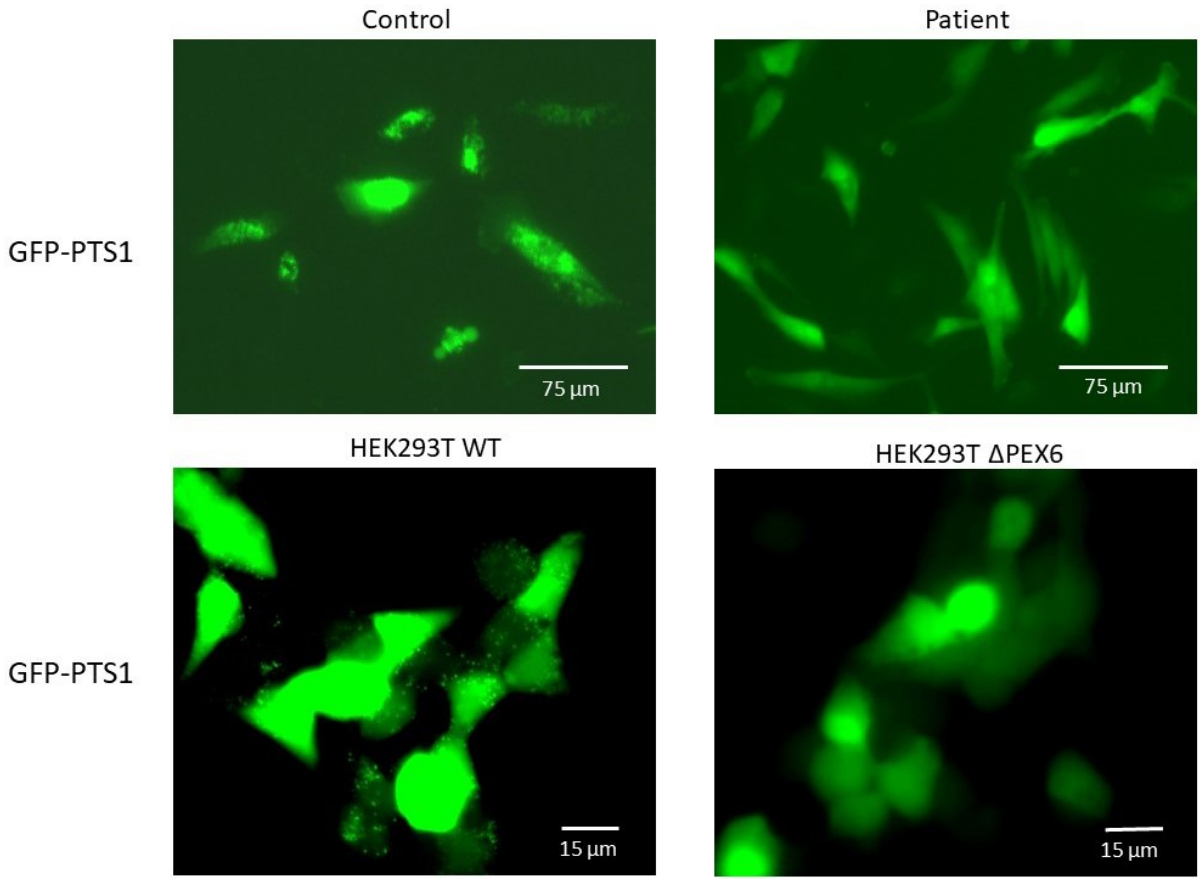

Figure 10. Microscopic images of *in vivo* GFP-PTS1 expression in fibroblasts and HEK293T cells. Cells were transfected with GFP-labelled PTS1 to interrogate the competency of peroxisomal matrix protein import. Control fibroblasts and wild-type HEK293T cells demonstrate intracellular punctate GFP signal, suggesting appropriate PTS1-mediated targeting of proteins to peroxisomes. The patient fibroblasts and *PEX6* knock-out cells, however, demonstrate diffuse cytosolic GFP signal, suggesting impaired PTS1-mediated peroxisomal protein import.

9.5 Interrogating PTS2-mediated peroxisomal protein import by immunofluorescence

Since the *in vivo* study of GFP-PTS1 distribution suggested that the PTS1 protein import pathway was defective in patient fibroblasts and *PEX6* knock-out cells, we decided to evaluate protein import via the PTS2-mediated pathway (Figure 2). While the majority of peroxisomal matrix proteins are imported via the PTS1 pathway, the PTS2 pathway is required for the import of several proteins, including thiolase, an enzyme involved in the peroxisomal β-oxidation pathway.[55] Analyzing both thiolase and Pex14 distribution by immunofluorescence would allow for an evaluation of the integrity of PTS2-mediated protein import and ensure that any intracellular punctate signal arises from peroxisomes by assessing thiolase and Pex14 co-localization. This confirmation of peroxisomal localization was not possible with the previous GFP-PTS1 *in vivo* assay.

In control fibroblasts, thiolase demonstrated an intracellular punctate distribution that co-localized with Pex14, the peroxisomal membrane marker that was used in the previous western blot assays. This suggested that the control fibroblasts have appropriate PTS2-mediated protein import. The patient fibroblasts, however, demonstrated a more diffuse, cytosolic, thiolase pattern with few intracellular puncta visible. Notably, the patient fibroblasts had a Pex14 distribution and abundance that resembled the control fibroblasts on immunofluorescence. The diffuse thiolase pattern evident in the patient fibroblasts suggested impaired PTS2-mediated peroxisomal protein import (Figure 11).

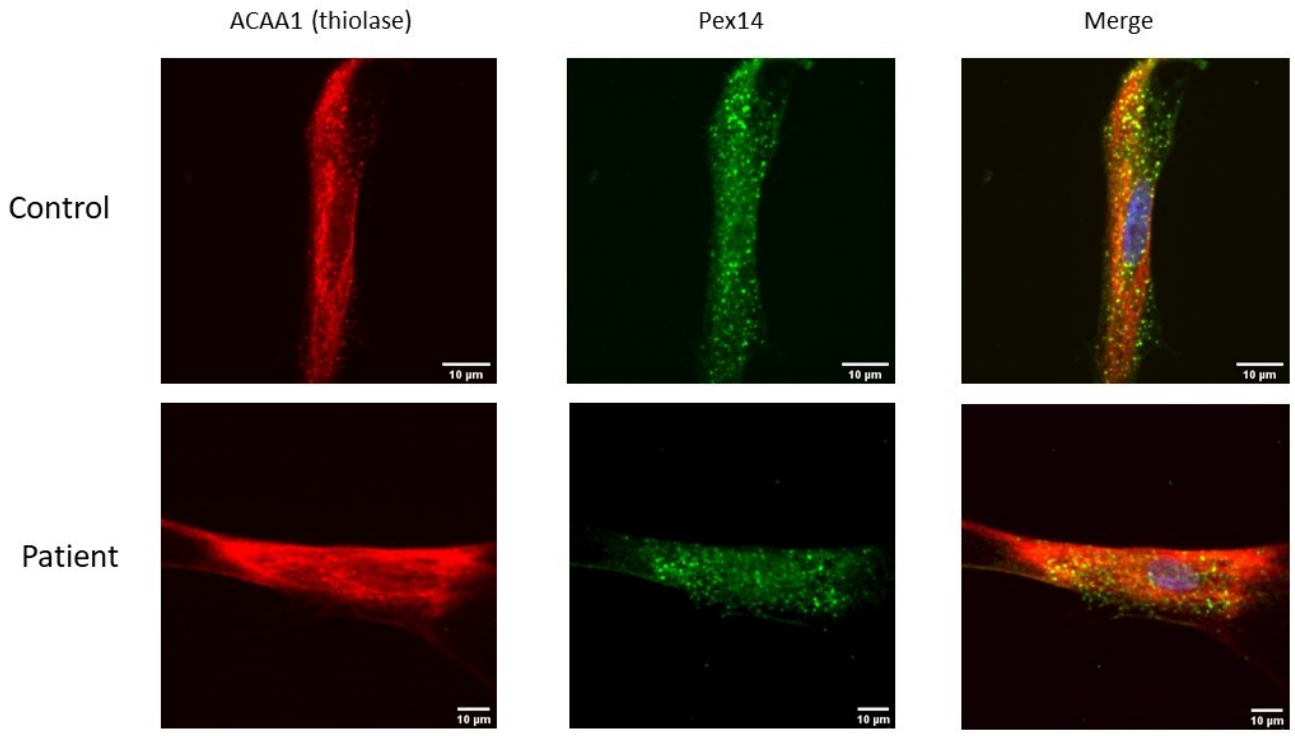

Figure 11. Immunofluorescence images of skin fibroblasts from control and patient sources. Thiolase, a protein imported via a PTS2-mediated process, demonstrates intracellular punctate localization that overlaps with Pex14, a peroxisomal membrane protein, suggesting appropriate PTS2-mediated targeting of proteins to peroxisomes in control fibroblasts. However, the patient fibroblasts demonstrate a more diffuse cytosolic thiolase localization with few puncta, despite a normal distribution of Pex14, suggesting impaired PTS2-mediated peroxisomal protein import.

To evaluate the PTS2-mediated protein import pathway in the CRISPR/Cas9-mediated *PEX6* knock-out HEK293T cells, a similar immunofluorescence assay was performed and the cellular distribution of thiolase and Pex14 was determined in HEK293T cells. In wild-type cells, thiolase demonstrated a punctate intracellular pattern that co-localized with Pex14, similar to the pattern evident in control fibroblasts, suggesting an intact PTS2-mediated protein import pathway. The *PEX6* knock-out cells, however, demonstrated a more diffuse, cytosolic, thiolase distribution similar to the pattern present in the patient fibroblasts, suggesting impaired PTS2 protein import. In the *PEX6* knock-out cells, there were fewer Pex14-labelled puncta compared to wild-type cells, and the few puncta that were present clustered around the cell nucleus (Figure 12).

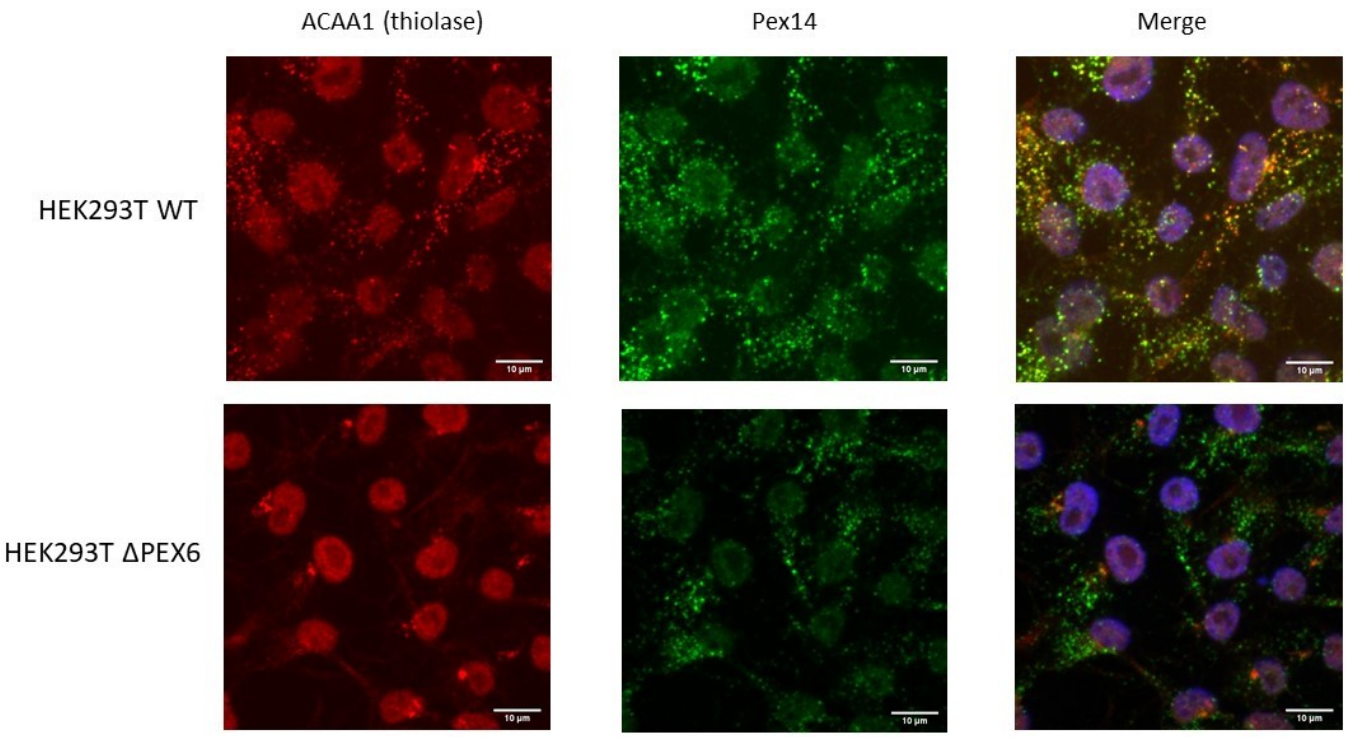

Figure 12. Immunofluorescence images of HEK293T wild-type cells and *PEX6* knock-out cells. Thiolase, a protein imported via a PTS2-mediated process, demonstrates intracellular punctate localization that overlaps with Pex14, a peroxisomal membrane protein, suggesting appropriate PTS2-mediated targeting of proteins to peroxisomes in wild-type cells. The *PEX6* knock-out cells, however, demonstrate a more diffuse cytosolic thiolase localization with few puncta localized in a peculiar perinuclear distribution, suggesting impaired PTS2-mediated peroxisomal protein import. There are also fewer Pex14-labelled puncta in the knock-out cells, consistent with reduced peroxisome abundance.

9.6 The processing of PTS2-thiolase confirmed defects in protein import in patient fibroblasts and *PEX6* knock-out cells

Thiolase exists as a 44 kDa protein with an N-terminal nonapeptide PTS2 sequence. Thiolase is recognized by Pex7, a protein crucial in targeting PTS2-containing proteins to the peroxisome, and together this complex is shuttled to the peroxisomal membrane aided by cytosolic Pex5.[35] Once thiolase reaches its destination in the peroxisomal lumen, the N-terminal PTS2 is enzymatically cleaved, leaving behind a 41 kDa thiolase protein (Figure 2).

In the control fibroblasts, the father's fibroblasts, and the mother's fibroblasts, the majority of thiolase is evident as a 41 kDa band on a western blot, suggesting appropriate peroxisomal localization as the PTS2 signal has been presumably cleaved off. In the patient fibroblasts, however, there is a band visible at 44 kDa, in addition to the thiolase band at 41 kDa, suggesting the presence of some uncleaved, and thus mislocalized, thiolase (Figure 13).

Similar to control fibroblasts, wild-type HEK293T cells show a thiolase band at 41 kDa, suggesting that thiolase is correctly localized to the peroxisome and that the PTS2 signal has been cleaved. In contrast, the *PEX6* knock-out cells show little thiolase at 41 kDa; the majority of detected protein is at 44 kDa on a western blot, suggesting mislocalization of thiolase and retention of the N-terminal PTS2 signal (Figure 13).

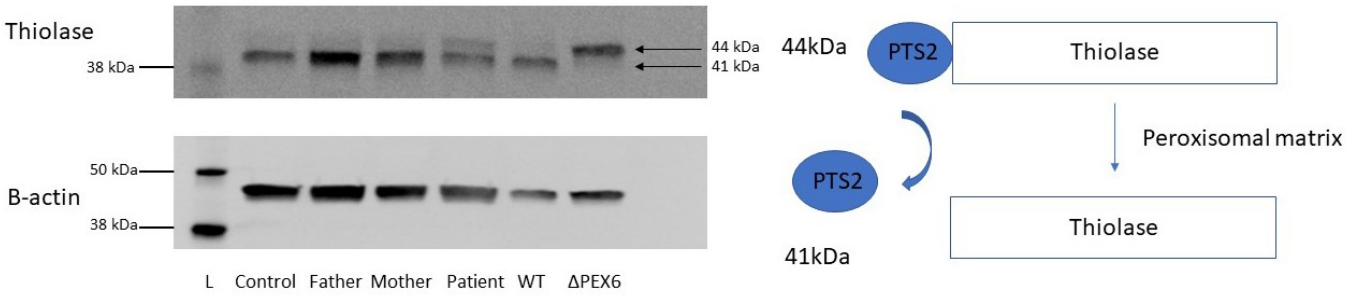

Figure 13. Processing of thiolase in skin fibroblasts and HEK293T cells on immunoblot. Thiolase, a protein imported into the peroxisomal matrix via a PTS2-mediated pathway, exists as a 44 kDa protein with its nonapeptide N-terminal PTS2 sequence. Once localized to the peroxisomal matrix, the PTS2 signal is cleaved, leaving behind a 41 kDa thiolase protein. In control fibroblasts, father's fibroblasts, and mother's fibroblasts, the majority of thiolase exists in its cleaved state, suggesting appropriate peroxisomal localization. In the patient fibroblasts, there is a visible thiolase band at the 44 kDa level, suggesting the presence of some uncleaved thiolase as a result of mislocalization. Wild-type HEK293T cells (WT) have the majority of thiolase existing in the cleaved state, compared to *PEX6* knock-out cells where the majority of thiolase is uncleaved, suggesting mislocalization. L = ladder (protein size standard).

9.7 Wild-type *PEX6* replacement rescues some PTS2 protein import in *PEX6* knock-out cells

To determine whether the protein import defect in *PEX6*-deficient cells could be rescued by introducing wild-type copies of *PEX6*, *PEX6* knock-out cells were transfected with wild-type FLAG-tagged *PEX6*. The HEK293T cells were selected over the fibroblasts for the initial assay as they are considerably easier to transfect and the difference in thiolase processing between wild-type and *PEX6* knock-out cells is greater compared to control and patient fibroblasts.

HEK293T *PEX6* knock-out cells were transfected with a FLAG-tagged *PEX6* expression plasmid. After 72 hours, thiolase processing was evaluated on a western blot as described above. *PEX6* over-expression in the *PEX6* knock-out cells resulted in the appearance of a 41 kDa thiolase band, suggesting that some thiolase was reaching the peroxisomal matrix and being processed. The ratio of processed to unprocessed thiolase was significantly increased following *PEX6* over-expression; it was determined to be 29% of that of wild-type HEK293T cells (P = 0.01; n = 2) (Figure 14).

9.8 *PEX6* c.35T>C over-expression rescues PTS2 protein import similar to wild-type *PEX6* replacement

Our patient with a peroxisomal biogenesis disorder had compound heterozygous changes in *PEX6* (c.802_815del/c.35T>C). The 14 base pair deletion was expected to lead to a frameshift and subsequent nonsense-mediated mRNA decay. The way in which the missense mutation, c.35T>C, leads to aberrant peroxisome function is not known. To investigate how the missense

variant affects protein import, a FLAG-tagged *PEX6* c.35T>C expression plasmid was generated by site-directed mutagenesis and transfected into HEK293T *PEX6* knock-out cells.

Similar to wild-type *PEX6* over-expression, *PEX6* c.35T>C over-expression resulted in a 41 kDa thiolase band on a western blot, suggesting that some PTS2-mediated peroxisomal protein import was restored. The ratio of processed to unprocessed thiolase was significantly increased following transfection with the *PEX6* missense variant compared to cells receiving an empty vector ($P = 0.01$; n = 3). The processing of thiolase was determined to be 27% of wild-type HEK293T cells, which was not significantly different from wild-type *PEX6* over-expression (Figure 14).

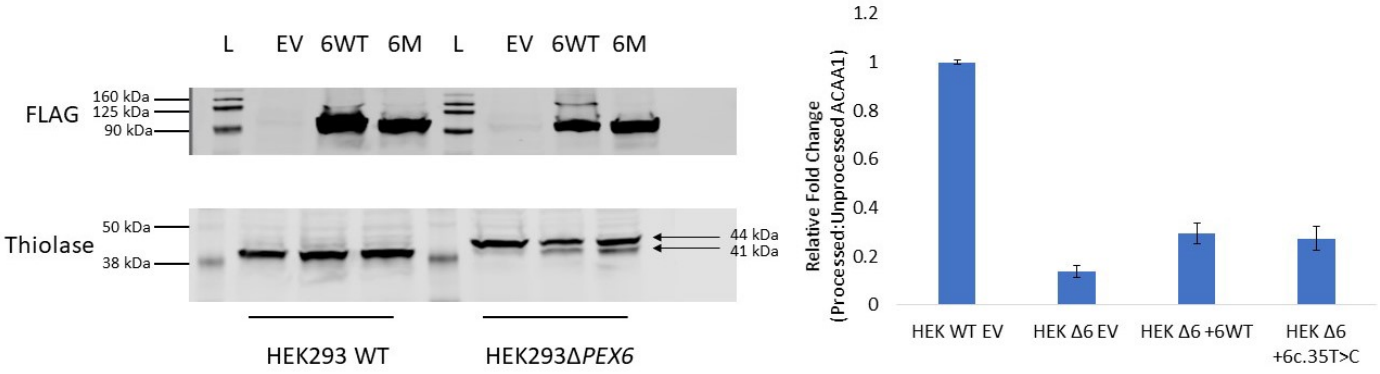

Figure 14. *PEX6* over-expression in HEK293T wild-type and *PEX6* knock-out cells. A FLAG-tagged *PEX6* expression plasmid was transfected into HEK293T cells, resulting in an approximately 40-fold increase in Pex6 levels. Both wild-type *PEX6* (6WT) and *PEX6* c.35T>C (6M) over-expression resulted in some thiolase cleavage compared to *PEX6* knock-out cells receiving the empty vector (EV), suggesting the rescue of some PTS2-mediated peroxisomal protein import with *PEX6* over-expression (HEK293 Δ*PEX6* EV vs 6WT; $P = 0.01$; n = 2 experimental replicates). Both *PEX6* wild-type and *PEX6* c.35T>C over-expression increased the ratio of processed to unprocessed thiolase (ACAA1) to nearly 30% of wild-type levels. L = ladder (protein size standard).

9.9 Over-expression of the cytosolic shuttle, Pex5, does not restore peroxisomal protein import in *PEX6* knock-out cells

Pex6 plays a role in extracting the cytosolic shuttle, Pex5, from the peroxisomal membrane for subsequent rounds of protein import.[36] Since peroxisomal membrane import, by both PTS1- and PTS2-mediated pathways, is disrupted in HEK293T *PEX6* knock-out cells and patient fibroblasts with *PEX6* mutations, presumably due to retained membrane-bound Pex5, we evaluated whether *PEX5* over-expression could overcome this import defect.

FLAG-tagged *PEX5* was transfected into HEK293T *PEX6* knock-out cells, and the processing of thiolase was evaluated after 72 hours. *PEX5* over-expression did not lead to any thiolase cleavage, with no protein band evident at 41kDa, suggesting that *PEX5* over-expression is unable to rescue PTS2-mediated peroxisomal protein import in cells devoid of Pex6 (Figure 15).

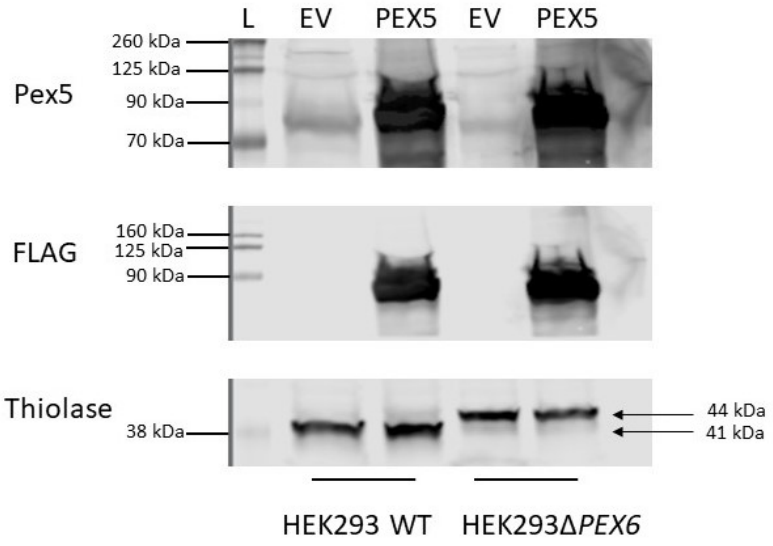

Figure 15. *PEX5* over-expression in HEK293T wild-type and *PEX6* knock-out cells. A FLAG-tagged *PEX5* (long isoform) expression plasmid was transfected into HEK293T cells, resulting in an approximately 15-fold increase in Pex5 levels. *PEX5* over-expression in *PEX6* knock-out cells does not lead to any thiolase cleavage, suggesting that *PEX5* over-expression is unable to rescue PTS2-mediated peroxisomal protein import in cells devoid of Pex6. L = ladder (protein size standard).

DISCUSSION

10.1 Revisiting peroxisomes and the retina

While evidence for the existence of peroxisomes in the retina has been available since the 1970s,[56] the precise role of peroxisomes in both healthy and diseased states of the retina remains obscure. A contributing factor may lie in the difficulty clinicians have in identifying patients with peroxisomal disorders due to significant phenotypic heterogeneity and the fact that many features overlap with more common diseases such as Usher syndrome and Leber congenital amaurosis (LCA).[46] In addition, many peroxisomal disorders are fatal in early infancy, making studies of retinal function problematic. With advances in molecular genetic testing, patients are now being offered more precise diagnoses and may be re-labelled as having a PBD when a peroxisomal disorder may not have been initially suspected.[46] By identifying more cases, new opportunities may arise to study PBDs, including milder forms, such as in our study, and this is anticipated to lead to an expanded understanding of peroxisome function.

10.2 Zellweger syndrome spectrum: infantile Refsum disease

Our patient presented with severe congenital SNHL and an early-onset retinal dystrophy. In the absence of other characteristic phenotypic findings, it would be difficult to make a diagnosis of a peroxisomal disorder. Based on these findings alone, he would have likely been labelled as having a variant of Usher syndrome, the most common cause of combined deafness and blindness. Fortunately, given that molecular genetic testing was available, bi-allelic mutations in

PEX6 were identified and he was subsequently diagnosed with a PBD. This led to an additional work-up, including a brain MRI, that demonstrated a leukodystrophy characteristic of a peroxisomal disorder. When considering the PBD disease spectrum, he likely falls within the infantile Refsum disease category since his overall presentation is milder. Additionally, the presence of neurologic changes and the absence of enamel and nail disease make a diagnosis of Heimler syndrome less likely.[57]

Given our patient's overall milder phenotypic manifestations, his age and ability to participate in additional clinical testing provided an opportunity to study his peroxisomal function. Our initial hypothesis was based on a recent study that demonstrated reduced peroxisome abundance, due to excessive pexophagy, in cells devoid of Pex1 or Pex26.[37] In particular, the authors demonstrated that both peroxisome number and matrix protein import could be recovered *in vitro* when cells were treated with chloroquine. This finding was of particular interest to us since chloroquine is a drug that is already used clinically both as an anti-malarial agent and an anti-inflammatory agent. In addition, the authors had not evaluated cells devoid of Pex6. Since Pex1, Pex6, and Pex26 belong to the same receptor/exportomer module, we hypothesized that Pex6 mutations would also lead to reduced peroxisome abundance via unchecked pexophagy.

10.3 Peroxisome abundance is reduced in *PEX6* knock-out cells but not in patient fibroblasts

To test this hypothesis, we obtained skin fibroblasts from the patient who harbored bi-allelic mutations in *PEX6* (c.802_815del/c.35T>C) and from his unaffected *PEX6* heterozygous father (WT/c.802_815del) and unaffected *PEX6* heterozygous mother (WT/c.35T>C). In concert, we

developed a homozygous *PEX6* knock-out line in HEK293T cells to emulate a more severe peroxisomal phenotype (c.544delG/c.544delG). Despite the patient's skin fibroblasts demonstrating significantly reduced endogenous levels of Pex6 protein on western blot (Figure 5), we did not detect a difference in peroxisome number using a surrogate marker of peroxisome abundance, Pex14 (Figure 6). This was further confirmed on a western blot using a second marker of peroxisome abundance, Pmp70/ABCD3 (Supplementary Figure 1). Pmp70 is a 70-kDa integral membrane protein that functions to transport lipids across the peroxisomal membrane.[37] This is the same marker utilized by Law *et al.* (2017) in their siRNA study of HeLa cells devoid of Pex1 and Pex26. We found Pex14 to be a more consistent and reliable peroxisomal marker than Pmp70, which tends to fluctuate in abundance and distribution depending on the metabolic state of the cell.[54] Although not quantified, the relative amount and distribution of Pex14 by immunofluorescence did not remarkably differ between control fibroblasts and patient fibroblasts, in keeping with the western blot data (Figure 11).

In the *PEX6* knock-out HEK293T cells, recapitulating a more severe Zellweger syndrome-like peroxisomal phenotype, there was essentially no detectable Pex6 protein on western blot (Figure 7). Unlike the patient fibroblasts, there was a significant reduction in Pex14 evident on western blot, suggesting reduced peroxisome abundance in the knock-out cells (Figure 9). In *PEX6* knock-out cells, Pex14 levels were 59% of Pex14 levels in wild-type HEK293T cells. This reduction in peroxisome abundance was comparable to what was reported in *PEX1* and *PEX26* siRNA experiments in HeLa cells.[37]

To further characterize the *PEX6* knock-out HEK293T cells at a protein level, we assessed the abundance of the other receptor/exportomer module components, Pex1 and Pex26. Pex1, which forms a heterohexameric complex with Pex6, was found to exist in similar amounts in *PEX6* knock-out and control cells, suggesting that the abundance of Pex1 does not depend on the presence or absence of Pex6 (Figure 8).[36] Pex26, an integral membrane protein that anchors the Pex1 and Pex6 heterohexameric complex to the peroxisomal membrane through interactions with Pex6, was found to be reduced by 60% in *PEX6* knock-out cells compared to control cells (Figure 8). This reduction was comparable to the decreased levels of Pex14, an integral membrane protein and surrogate for peroxisome abundance, demonstrated in the *PEX6* knock-out cells. We hypothesized that the reduced levels of Pex26, like Pex14 and Pmp70, may also reflect reduced peroxisomal abundance in cells devoid of Pex6, given that these are all intrinsic peroxisomal membrane proteins.

Given that we did not find evidence to suggest reduced peroxisome abundance in patient fibroblasts containing compound heterozygous mutations in *PEX6*, our initial hypothesis was not confirmed. As a result, we did not explore further the effect of adding chloroquine to cultured fibroblasts. A possible reason for why our results differed from findings in the study by Law *et al.* (2017) may be due to the nature of mutation in the peroxisomal genes. Our patient had a 14 base-pair deletion on one of the *PEX6* alleles; this deletion would be anticipated to lead to nonsense-mediated mRNA decay. The other *PEX6* allele is a missense mutation, c.35T>C, and changes a phenylalanine residue to a serine residue at position 12 in the primary amino acid sequence. While the precise effect of the missense mutation is unknown, it predictably would be less damaging to the protein structure and function than the 14 base-pair deletion. This is

supported by our patient's milder phenotype compared to a more severe Zellweger syndrome in patients with the same homozygous 14 base-pair deletion.[52] We hypothesize that a certain amount of residual Pex6 protein is enough to prevent aberrant pexophagy.

In the study by Law *et al.* (2017), HeLa cells were transfected with *PEX1* and *PEX26* siRNA, and the resulting protein levels were considerably reduced. This is analogous to what we achieved in our *PEX6* knock-out HEK293T cells, where we also found reduced peroxisome abundance (Figure 9). While we did not evaluate whether the reduced peroxisome abundance resulted from excessive peroxisomal degradation in our knock-out cells, this idea is plausible and would support the findings from the above study.[37] Although it is possible that Pex6 does not influence peroxisome turnover and pexophagy, we believe that excessive peroxisomal degradation may be a feature of deleterious (i.e. nonsense) mutations in *PEX1*, *PEX6*, and *PEX26*, and contribute to a more severe disease phenotype.

10.4 PTS1-mediated peroxisomal matrix protein import is impaired in patient fibroblasts and *PEX6* knock-out cells

Since peroxisome abundance was not altered in the patient's fibroblasts, we evaluated whether the cells were deficient in peroxisomal matrix protein import, one of the other main roles of Pex6.[35] We separately evaluated the two pathways of peroxisomal matrix protein import: the PTS1 and PTS2 pathways (Figure 2). We found that patient fibroblasts transfected with GFP-PTS1 displayed a diffuse, cytosolic GFP signal with no discernible punctate structures. This differed from control fibroblasts where punctate GFP-labelled structures were evident (Figure

10). Since this was an *in vivo* experiment with a single transfected construct, we were unable to confirm whether the punctate structures evident in the control fibroblasts were, in fact, peroxisomes, but we utilized a commercially available expression plasmid that had been previously validated.[58] Using the same GFP-PTS1 expression plasmid in *PEX6* knock-out HEK293T cells, we found that the knock-out cells also had a diffuse, cytosolic GFP signal compared to control cells (Figure 10). These findings in both fibroblasts and HEK293T cells provide evidence to support impaired PTS1-mediated peroxisomal matrix protein import in cells with *PEX6* mutation. While the complete absence of Pex6 may alter peroxisome abundance, both patient fibroblasts (with some residual Pex6) and *PEX6* knock-out cells demonstrated aberrant PTS1-mediated protein import.

10.5 PTS2-mediated peroxisomal matrix protein import is impaired in patient fibroblasts and *PEX6* knock-out cells

To interrogate PTS2-mediated peroxisomal protein import, we performed immunofluorescence studies on patient fibroblasts using an antibody against thiolase, a protein imported by the PTS2 pathway, and an antibody against Pex14, to label peroxisomes (Figure 2). In patient fibroblasts, thiolase demonstrated a more diffuse cytosolic pattern with only a few punctate structures evident that co-localized with Pex14 (Figure 11). This was in contrast to control fibroblasts, where thiolase demonstrated a punctate localization that overlapped with Pex14. This co-localization in control fibroblasts indicated that thiolase was, indeed, appropriately labelling peroxisomes, as indicated by Pex14 (Figure 11). Reduced thiolase-labelled puncta in patient fibroblasts along with increased cytosolic signal suggested that thiolase was not being targeted to

peroxisomes or imported into the peroxisomal matrix effectively. These results are consistent with the findings in the GFP-PTS1 transfected fibroblasts and they are in keeping with a generalized defect in peroxisomal protein import in patient fibroblasts with *PEX6* mutation.

Utilizing the same antibodies and immunofluorescence assay, *PEX6* knock-out HEK293T cells also demonstrated a diffuse cytosolic thiolase pattern with only a few punctate structures evident in a perinuclear distribution (Figure 12). In addition, there were fewer Pex14-labelled puncta in the knock-out cells, consistent with the reduced peroxisomal abundance that we previously described for a western blot (Figure 9). Moreover, these Pex14-labelled puncta also occurred in a perinuclear distribution. There was little co-localization of thiolase and Pex14 in the knock-out cells. This finding suggests that the Pex14-labelled structures are import-incompetent or so-called "ghost" peroxisomes, previously described in other PBDs.[59-61]

To support our finding of impaired peroxisomal matrix protein import evident by cell imaging in patient fibroblasts and *PEX6* knock-out cells, we evaluated the processing of thiolase on a western blot. Thiolase is a protein targeted to the peroxisomal matrix via a PTS2-mediated import process (Figure 2). Once in the matrix, the enzyme Tysnd1 cleaves the N-terminal PTS2 signal from thiolase.[62] The difference in molecular size between processed/cleaved and unprocessed/uncleaved thiolase can be resolved on a western blot. In agreement with the *in vivo* GFP-PTS1 assay and the PTS2 immunofluorescence experiment, patient fibroblasts demonstrated some uncleaved thiolase, suggesting that thiolase was not reaching the peroxisomal matrix (Figure 13). While it was difficult to assess the degree of residual peroxisomal protein import by the cell imaging assays, the presence of some cleaved thiolase in the patient fibroblasts

supports the existence of residual protein import and explains the milder phenotype in our patient. Both of the patient's parents had a pattern of thiolase processing that was the same as that of control fibroblasts (Figure 13). Consistent with a more severe peroxisomal phenotype, there was little, if any, cleaved thiolase evident in the *PEX6* knock-out HEK293T cells (Figure 13). This logically follows the absence of Pex6 protein in these cells as the presence of at least some Pex6 is critical for matrix protein import.[35]

10.6 Comparison of our findings to previous studies of patients with *PEX6* mutations

Taken together, our results demonstrate that fibroblasts from our patient with compound heterozygous mutations in *PEX6* (c.802_815del/c.35T>C) have reduced peroxisomal import capacity but do not have altered peroxisome abundance. Mutations in *PEX6* were identified in 1996 to cause a peroxisomal biogenesis disorder in humans.[63] Fibroblasts from patients with severe Zellweger syndrome demonstrated a cytosolic distribution of catalase on immunofluorescence; a punctate peroxisomal distribution of catalase ensued when cells were complemented with human *PEX6* cDNA.[63] These cells were clearly import-incompetent; however, the abundance of peroxisomes had not been assessed. Later, another group examined the amount of Pex14 and Pmp70 in fibroblasts from a patient with Zellweger syndrome due to biallelic *PEX6* frameshift mutations. The authors reported reduced peroxisome abundance to less than 20% that of control fibroblasts.[64] Finally, fibroblasts from a patient with missense mutations in *PEX6* and a milder clinical phenotype of neonatal adrenoleukodystrophy demonstrated a temperature-sensitive mosaic phenotype where import-incompetent peroxisomes became import-competent when the cells were incubated at a reduced temperature.[65]

10.7 Mechanism of disease and cellular phenotype may depend on the nature of *PEX6* mutation

Our results highlight that the nature of mutation in *PEX6* can influence the peroxisomal phenotype evident in fibroblasts and the resulting disease severity. We hypothesize that the presence of hypomorphic or missense mutations in *PEX6* lead to reduced matrix protein import but not to reduced peroxisome abundance, as suggested by our fibroblast data. Furthermore, we suspect that more deleterious mutations in *PEX6* would lead to both reduced matrix protein import and reduced peroxisome abundance. This combination of defects in peroxisome biogenesis or pexophagy and matrix protein import results in a more severe disease phenotype.

This distinction may have important therapeutic implications. For example, the chemical chaperone arginine has been shown to improve matrix protein import in fibroblasts from a patient with a mild PBD due to *PEX6* mutation.[66] Although we did not assess the effect of temperature on peroxisome protein import in our patient fibroblasts, milder *PEX6* PBDs have been found to have reduced protein import when cells are exposed to higher temperatures.[25] This has been attributed to the destabilizing effect of missense mutations on the Pex6 protein.[25] As a result, chemical chaperones, such as arginine, may stabilize Pex6 and rescue some import activity in mild PBDs. Consistent with this, a patient with *PEX12* mutations was treated with L-arginine and demonstrated improved serum biochemical parameters and improved hearing.[67] On the other hand, chemical chaperones may not be expected to result in significant improvement in patients with more severe disease due to both impaired protein import and reduced peroxisome

abundance. In these instances, drugs such as chloroquine, a lysosomal alkalinizer, demonstrates promise in reducing excessive peroxisomal degradation.[37]

10.8 *PEX6* over-expression can rescue peroxisomal matrix protein import in *PEX6* knock-out cells

To investigate genetic approaches to improve impaired peroxisome protein import, we performed two experiments on the *PEX6* knock-out HEK293T cells. In the first, we determined whether over-expressing wild-type *PEX6* in *PEX6* knock-out cells might rescue peroxisome function by assessing thiolase processing on western blot. In tandem, we transfected *PEX6* knock-out cells with a plasmid containing the *PEX6* c.35T>C variant to evaluate whether it was capable of promoting matrix protein import. Over-expressing both the wild-type *PEX6* and *PEX6* c.35T>C each resulted in a similar improvement in the processing of thiolase in *PEX6* knock-out cells to nearly 30% that of *PEX6* wild-type cells (Figure 14). In addition to highlighting a potential role for *PEX6* over-expression in recovering peroxisome function, this assay also provided evidence to show that *PEX6* c.35T>C still has some protein import capacity. In the second experiment, we evaluated whether over-expressing *PEX5*, the peroxisomal cytosolic shuttle, could rescue protein import in *PEX6* knock-out cells. Since Pex6 facilitates protein trafficking by releasing Pex5 from the peroxisomal membrane for subsequent rounds of protein import (Figure 2), we questioned if over-expressing Pex5 might increase its cytosolic concentration and enable some peroxisome protein import to occur in the absence of Pex6. We found, however, that *PEX5* over-expression was not able to rescue any thiolase processing, and thus protein import, in *PEX6* knock-out cells

(Figure 15). This supports the conclusion that the presence of at least some Pex6 is required for peroxisome protein import.

10.9 Future directions

Our future experiments will seek to determine the effect of temperature on peroxisome matrix protein import in our patient fibroblasts. We suspect that incubating the fibroblasts at 40C, as opposed to 37C, will further reduce matrix protein import, supporting the hypothesis that milder PBD phenotypes involve reduced peroxin stability. In addition, we will perform a cycloheximide chase assay to determine whether the missense variant *PEX6* c.35T>C leads to reduced Pex6 protein stability in HEK293T cells transfected with FLAG-tagged *PEX6* c.35T>C constructs compared to FLAG-tagged *PEX6* wild-type constructs. We hypothesize that the *PEX6* c.35T>C variant will lead to reduced Pex6 protein stability. If present, this reduced Pex6 protein stability in patient fibroblasts and in transfected HEK293T cells may be partially restored with arginine supplementation.[66]

In addition, we would be interested in determining whether we can improve peroxisome function by assessing thiolase processing and PTS1 and PTS2 protein import on immunofluorescence by over-expressing wild-type *PEX6* in patient fibroblasts. We would anticipate that at least some peroxisome protein import would be restored. To follow the *PEX5* over-expression assay in *PEX6* knock-out HEK293T cells, a future experiment may be to over-express *PEX5* in the patient fibroblasts and assess whether protein import can be rescued. Unlike the *PEX6* knock-out cells, the patient fibroblasts have residual Pex6 protein so it may be possible to recover some

matrix protein import in patient fibroblasts by increasing the cytoplasmic concentration of Pex5. Enhancing Pex5 in the cytoplasm may overcome the deficient protein import that is limited in patient fibroblasts by Pex5 being retained on the peroxisome membrane and not being released into the cytosol by Pex6 for subsequent rounds of protein import. Finally, we plan on determining whether chloroquine can rescue peroxisome number and protein import in the *PEX6* knock-out HEK293T cells. Our *PEX6* knock-out cell line recapitulates the *PEX1* and *PEX26* knock-down HeLa cells by Law *et al.* (2017) in that each cell line is devoid of its respective peroxin. Since improved protein abundance, due to reduced pexophagy, and improved protein import occurred in cells treated with chloroquine, we suspect that a similar finding may occur in our *PEX6* knock-out cells.[37] If present, this finding would emphasize the potential utility of chloroquine as a therapeutic agent for PBDs with severe mutations leading to little remaining peroxin protein.

Although we have evaluated how specific mutations in *PEX6* affect peroxisome function in patient fibroblasts, we have yet to explore how these changes specifically affect retinal function. In the future, we will aim to generate patient fibroblast-derived induced pluripotent stem cells (iPSCs) and differentiate these into RPE cells. We plan on conducting an assay to determine the effect of *PEX6* mutations on RPE-mediated photoreceptor outer segment phagocytosis, as this is one of the proposed roles of peroxisomes in the RPE.[49] Studies such as this in retina-specific cells will provide insight into how peroxisomes function in the retina. In addition, individualized iPSC-RPE cells would act as a model to evaluate the potential for future gene augmentation strategies in patients with PBDs.

10.10 Study limitations

One of the limitations of our study is that we evaluated the effect of patient-specific *PEX6* mutations in skin fibroblasts. Numerous other studies have similarly evaluated PBDs in skin fibroblasts;[25,68-70] however, cutaneous manifestations of disease are not typical of PBDs.[23] Skin fibroblasts are readily obtained via a superficial dermal punch biopsy. As a result, the convenience of establishing a primary cell line in culture with patient-specific mutations makes the use of skin fibroblasts attractive. However, there is significant heterogeneity in the gene expression profile of different tissue types; 50% of all genes demonstrate tissue-specific expression.[71] Since peroxisomes are ubiquitous organelles, skin fibroblasts may be an acceptable model to evaluate peroxisome function in general. However, to evaluate tissue-specific effects of peroxisome dysfunction, such as in the retina, it would be important to utilize a model such as iPSC-RPE cells which demonstrate similar membrane potential, ion transport, and gene expression profiles as native RPE.[72]

Despite our study demonstrating reduced peroxisomal protein import in patient fibroblasts with mutations in *PEX6*, an additional limitation is that we did not explicitly evaluate the consequence of this impaired protein import on the major functions of the peroxisome. We would expect that reduced protein import in the patient fibroblasts would result in aberrant peroxisomal function. DHA, a polyunsaturated fatty acid that exists as a major structural lipid in the retina,[73] is synthesized in the endoplasmic reticulum and further processed by β-oxidation reactions in peroxisomes.[74] Both levels of DHA-containing phospholipids and β-oxidation activity can be

measured by liquid chromatography/mass spectrometry.[68] An experiment such as this would allow for a read-out of peroxisome function in our patient fibroblasts.

Finally, our study is limited by the analysis of a single PBD patient. Thus far, our patient is the only one in our clinic who has a confirmed PBD diagnosis. Although peroxisomal disorders are reportedly rare,[75] the actual prevalence may be higher with more widespread availability of genetic testing that can molecularly solve cases that overlap considerably with other disorders.[76] Although conclusions made in a single patient cannot necessarily be generalized to all patients with peroxisomal disorders, our findings of disrupted protein import and normal peroxisome abundance in our patient's fibroblasts demonstrate that specific mutations can have different effects on peroxisome metabolism. Moreover, the consequences of these mutations may require different therapeutic approaches. While observations in individual patients are important, we hope to gather additional samples from patients with *PEX6* mutations to further support our findings.

10.11 Concluding remarks

In conclusion, we have demonstrated that skin fibroblasts from a patient with compound heterozygous mutations in *PEX6* have abnormal peroxisomal matrix protein import but not abnormal peroxisomal abundance. This is in contrast to *PEX6* knock-out HEK293T cells, which demonstrate both a severe defect in matrix protein import and a significant reduction in peroxisome abundance. We hypothesize that the reduction in peroxisome abundance is a feature of the more severe phenotypes along the Zellweger syndrome spectrum and is likely due to

frameshift or nonsense mutations in *PEX* genes that result in little protein product. These differences become important when therapeutic approaches are considered and highlight the importance of understanding disease mechanisms on a patient-specific and mutation-specific level.

REFERENCES

1. Fuhrmann S, Zou C, Levine EM. Retinal pigment epithelium development, plasticity, and tissue homeostasis. *Exp Eye Res*. 2014;123:141-150.

2. Strauss O. The retinal pigment epithelium in visual function. *Physiol Rev*. 2005;85:845-881.

3. Chaum E, Winborn CS, Bhattacharya S. Genomic regulation of senescence and innate immunity signaling in the retinal pigment epithelium. *Mamm Genome*. 2015;26:210-21.

4. Dietrich L, Lucius R, Roider J, Klettner A. Interaction of inflammatorily activated retinal pigment epithelium with retinal microglia and neuronal cells. *Exp Eye Res.* 2020;28:108167.

5. Ebihara N, Chen L, Tokura T, Ushio H, Iwatsu M, Murakami A. Distinct functions between toll-like receptors 3 and 9 in retinal pigment epithelial cells. *Ophthalmic Res*. 2007;39:155-163.

6. Casey GA, Papp KM, MacDonald IM. Ocular Gene Therapy with Adeno-associated Virus Vectors: Current Outlook for Patients and Researchers. *J Ophthalmic Vis Res*. 2020;15:396-399.

7. “Anatomy and Physiology of the Retina”. Webvision. Moran Eye Center, October 8, 2011. Web. Accessed June 15, 2020. https://webvision.med.utah.edu/book/part-ii-anatomy-and-physiology-of-the-retina/oute-plexiform/

8. Diamond JS. Inhibitory Interneurons in the Retina: Types, Circuitry, and Function. *Annu Rev Vis Sci.* 2017;3:1-24.

9. Smith AM, Czyz CN. Neuroanatomy, Cranial Nerve 2 (Optic) [Updated 2020 Jul 31]. In: StatPearls [Internet]. Treasure Island (FL): StatPearls Publishing; 2020 Jan-. Available from: https://www.ncbi.nlm.nih.gov/books/NBK507907/

10. Arbabi A, Liu A, Ameri H. Gene Therapy for Inherited Retinal Degeneration. *J Ocul Pharmacol Ther.* 2019;35:79-97.

11. SP Daiger, BJF Rossiter, J Greenberg, A Christoffels, W Hide. Data services and software for identifying genes and mutations causing retinal degeneration. *Invest. Ophthalmol.Vis. Sci*. 1998;39:S295.

12. Verbakel SK, van Huet RAC, Boon CJF, den Hollander AI, Collin RWJ, Klaver CCW et al. Non-syndromic retinitis pigmentosa. *Prog Retin Eye Res.* 2018;66:157-186.

13. Dimopoulos IS, Hoang SC, Radziwon A, Binczyk NM, Seabra MC, MacLaren RE, et al. Two-Year Results After AAV2-Mediated Gene Therapy for Choroideremia: The Alberta

Experience. *Am J Ophthalmol*. 2018;193:130-142.

14. Russell S, Bennett J, Wellman JA, Chung DC, Yu ZF, Tillman A, et al. Efficacy and safety of voretigene neparvovec (AAV2-hRPE65v2) in patients with RPE65-mediated inherited retinal dystrophy: a randomised, controlled, open-label, phase 3 trial. *Lancet*. 2017;390:849-860.

15. Sadagopan KA. Practical approach to syndromic pediatric retinal dystrophies. *Curr Opin Ophthalmol.* 2017;28:416-429.

16. Fujiki Y, Abe Y, Imoto Y, Tanaka AJ, Okumoto K, Honsho M, et al. Recent insights into peroxisome biogenesis and associated diseases. *J Cell Sci.* 2020;133:jcs236943.

17. Pennesi ME, Weleber RG. (2012). Peroxisomal disorders. In: Trabousli EI, editor. *Genetic Diseases of the Eye: Second Edition* (pp. 712-741). Oxford Monographs of Medical Genetics.

18. Tan AP, Gonçalves FG, Almehdar A, Soares BP. Clinical and Neuroimaging Spectrum of Peroxisomal Disorders. *Top Magn Reson Imaging.* 2018;27:241-257.

19. Geisbrecht BV, Collins CS, Reuber BE, Gould SJ. Disruption of a PEX1-PEX6 interaction is the most common cause of the neurologic disorders Zellweger syndrome, neonatal

adrenoleukodystrophy, and infantile Refsum disease. *Proc Natl Acad Sci U S A*. 1998;95:8630-8635.

20. Wei H, Kemp S, McGuinness MC, Moser AB, Smith KD. Pharmacological induction of peroxisomes in peroxisome biogenesis disorders. *Ann Neurol*. 2000;47:286-296.

21. Barillari MR, Karali M, Di Iorio V, Contaldo M, Piccolo V, Esposito M, et al. Mild form of Zellweger Spectrum Disorders (ZSD) due to variants in *PEX1*: Detailed clinical investigation in a 9-years-old female. *Mol Genet Metab Rep*. 2020;24:100615.

22. Ventura MJ, Wheaton D, Xu M, Birch D, Bowne SJ, Sullivan LS, et al. Diagnosis of a mild peroxisomal phenotype with next-generation sequencing. *Mol Genet Metab Rep.* 2016;9:75-78.

23. Steinberg SJ, Raymond GV, Braverman NE, et al. Zellweger Spectrum Disorder. 2003 Dec 12 [Updated 2017 Dec 21]. In: Adam MP, Ardinger HH, Pagon RA, et al., editors. GeneReviews® [Internet]. Seattle (WA): University of Washington, Seattle; 1993-2020. Available from: https://www.ncbi.nlm.nih.gov/books/NBK1448/

24. Heimler A, Fox JE, Hershey JE, Crespi P. Sensorineural hearing loss, enamel hypoplasia, and nail abnormalities in sibs. *Am J Med Genet*. 1991;39:192-195.

25. Ratbi I, Falkenberg KD, Sommen M, Al-Sheqaih N, Guaoua S, Vandeweyer G, et al. Heimler Syndrome Is Caused by Hypomorphic Mutations in the Peroxisome-Biogenesis Genes PEX1 and PEX6. *Am J Hum Genet.* 2015;97:535-545.

26. Wangtiraumnuay N, Alnabi WA, Tsukikawa M, Thau A, Capasso J, Sharony R, et al. Ophthalmic manifestations of Heimler syndrome due to PEX6 mutations. *Ophthalmic Genet*. 2018;39:384-390.

27. Gao FJ, Hu FY, Xu P, Qi YH, Li JK, Zhang YJ, et al. Expanding the clinical and genetic spectrum of Heimler syndrome. *Orphanet J Rare Dis.* 2019;14:290.

28. Akiyama N, Ghaedi K, Fujiki Y. A novel pex2 mutant: catalase-deficient but temperature-sensitive PTS1 and PTS2 import. *Biochem Biophys Res Commun.* 2002;293:1523-1529.

29. Mast FD, Fagarasanu A, Knoblach B, Rachubinski RA. Peroxisome biogenesis: something old, something new, something borrowed. *Physiology (Bethesda)*. 2010;25:347-356.

30. Mast FD, Rachubinski RA, Aitchison JD. Peroxisome prognostications: Exploring the birth, life, and death of an organelle. *J Cell Biol.* 2020;219:e201912100.

31. De Duve C, Beaufay H, Jacques P, Rahman-Li Y, Sellinger OZ, Wattiaux R, et al. Intracellular localization of catalase and of some oxidases in rat liver. *Biochim Biophys Acta*. 1960;40:186-187.

32. Di Cara F, Sheshachalam A, Braverman NE, Rachubinski RA, Simmonds AJ. Peroxisome-Mediated Metabolism Is Required for Immune Response to Microbial Infection. *Immunity*. 2017;47:93-106.

33. Hettema EH, Motley AM. How peroxisomes multiply. *J Cell Sci.* 2009;122:2331-2336.

34. Honsho M, Yamashita S, Fujiki Y. Peroxisome homeostasis: Mechanisms of division and selective degradation of peroxisomes in mammals. *Biochim Biophys Acta*. 2016;1863:984-991.

35. Pedrosa AG, Francisco T, Ferreira MJ, Rodrigues TA, Barros-Barbosa A, Azevedo JE. A Mechanistic Perspective on PEX1 and PEX6, Two AAA+ Proteins of the Peroxisomal Protein Import Machinery. *Int J Mol Sci*. 2019;20:5246.

36. Dias AF, Francisco T, Rodrigues TA, Grou CP, Azevedo JE. The first minutes in the life of a peroxisomal matrix protein. *Biochim Biophys Acta*. 2016;1863:814-820.

37. Law KB, Bronte-Tinkew D, Di Pietro E, Snowden A, Jones RO, Moser A, et al. The peroxisomal AAA ATPase complex prevents pexophagy and development of peroxisome biogenesis disorders. *Autophagy*. 2017;13:868-884.

38. Lodhi IJ, Semenkovich CF. Peroxisomes: a nexus for lipid metabolism and cellular signaling.

Cell Metab. 2014;19:380-392.

39. Singh I, Moser AE, Goldfischer S, Moser HW. Lignoceric acid is oxidized in the peroxisome: implications for the Zellweger cerebro-hepato-renal syndrome and adrenoleukodystrophy. *Proc Natl Acad Sci U S A*. 1984;81:4203-4207.

40. Schönfeld P, Reiser G. Brain Lipotoxicity of Phytanic Acid and Very Long-chain Fatty Acids. Harmful Cellular/Mitochondrial Activities in Refsum Disease and X-Linked Adrenoleukodystrophy. *Aging Dis*. 2016;7:136-149.

41. van den Brink DM, Wanders RJ. Phytanic acid: production from phytol, its breakdown and role in human disease. *Cell Mol Life Sci*. 2006;63:1752-1765.

42. St Jules R, Setlik W, Kennard J, Holtzman E. Peroxisomes in the head of Drosophila melanogaster. *Exp Eye Res*. 1990;51:607-617.

43. St Jules R, Kennard J, Setlik W, Holtzman E. Frog cones as well as Müller cells have peroxisomes. *Exp Eye Res*. 1992;54:1-8.

44. Zaki MS, Heller R, Thoenes M, Nürnberg G, Stern-Schneider G, Nürnberg P, et al. PEX6 is expressed in photoreceptor cilia and mutated in deafblindness with enamel dysplasia and microcephaly. *Hum Mutat*. 2016;37:170-174.

45. Smith CE, Poulter JA, Levin AV, Capasso JE, Price S, Ben-Yosef T, et al. Spectrum of PEX1 and PEX6 variants in Heimler syndrome. *Eur J Hum Genet*. 2016;24:1565-1571.

46. Das Y, Roose N, De Groef L, Fransen M, Moons L, Van Veldhoven PP, et al. Differential distribution of peroxisomal proteins points to specific roles of peroxisomes in the murine retina. *Mol Cell Biochem*. 2019;456:53-62.

47. Deguchi J, Yamamoto A, Fujiki Y, Uyama M, Tsukahara I, Tashiro Y. Localization of nonspecific lipid transfer protein (nsLTP = sterol carrier protein 2) and acyl-CoA oxidase in peroxisomes of pigment epithelial cells of rat retina. *J Histochem Cytochem*. 1992;40:403-410.

48. Burgoyne T, Lane A, Laughlin WE, Cheetham ME, Futter CE. Correlative light and immuno-electron microscopy of retinal tissue cryostat sections. *PLoS One*. 2018;13:e0191048.

49. Daniele LL, Caughey J, Volland S, Sharp RC, Dhingra A, Williams DS, et al. Peroxisome turnover and diurnal modulation of antioxidant activity in retinal pigment epithelia utilizes microtubule-associated protein 1 light chain 3B (LC3B). *Am J Physiol Cell Physiol*. 2019;317:C1194-C1204.

50. Miceli MV, Liles MR, Newsome DA. Evaluation of oxidative processes in human pigment epithelial cells associated with retinal outer segment phagocytosis. *Exp Cell Res*. 1994;214:242-249.

51. O'Neal TB, Luther EE. Retinitis Pigmentosa. [Updated 2020 Aug 10]. In: StatPearls [Internet]. Treasure Island (FL): StatPearls Publishing; 2020 Jan-. Available from: https://www.ncbi.nlm.nih.gov/books/NBK519518/

52. Levesque S, Morin C, Guay SP, Villeneuve J, Marquis P, Yik WY, et al. A founder mutation in the PEX6 gene is responsible for increased incidence of Zellweger syndrome in a French Canadian population. *BMC Med Genet*. 2012;13:72.

53. Steinberg S, Chen L, Wei L, Moser A, Moser H, Cutting G, et al. The PEX Gene Screen: molecular diagnosis of peroxisome biogenesis disorders in the Zellweger syndrome spectrum. *Mol Genet Metab*. 2004;83:252-263.

54. Grant P, Ahlemeyer B, Karnati S, Berg T, Stelzig I, Nenicu A, et al. The biogenesis protein PEX14 is an optimal marker for the identification and localization of peroxisomes in different cell types, tissues, and species in morphological studies. *Histochem Cell Biol*. 2013;140:423-442.

55. Kunze M, Malkani N, Maurer-Stroh S, Wiesinger C, Schmid JA, Berger J. Mechanistic insights into PTS2-mediated peroxisomal protein import: the co-receptor PEX5L

drastically increases the interaction strength between the cargo protein and the receptor PEX7. *J Biol Chem*. 2015;290:4928-4940.

56. Leuenberger PM, Novikoff AB. Studies on microperoxisomes. VII. Pigment epithelial cells and other cell types in the retina of rodents. *J Cell Biol*. 1975;65:324-334.

57. Varela MD, Jani P, Zein WM, D'Souza P, Wolfe L, Chisholm J, et al. The peroxisomal disorder spectrum and Heimler syndrome: Deep phenotyping and review of the literature. *Am J Med Genet C Semin Med Genet*. 2020;184:618-630.

58. Sexton JZ, He Q, Forsberg LJ, Brenman JE. High content screening for non-classical peroxisome proliferators. *Int J High Throughput Screen*. 2010:127-140.

59. Santos MJ, Imanaka T, Shio H, Small GM, Lazarow PB. Peroxisomal membrane ghosts in Zellweger syndrome--aberrant organelle assembly. *Science*. 1988;239:1536-1538.

60. Santos MJ, Imanaka T, Shio H, Lazarow PB. Peroxisomal integral membrane proteins in control and Zellweger fibroblasts. *J Biol Chem*. 1988;263:10502-10509.

61. Soliman K, Göttfert F, Rosewich H, Thoms S, Gärtner J. Super-resolution imaging reveals the sub-diffraction phenotype of Zellweger Syndrome ghosts and wild-type peroxisomes. *Sci Rep*. 2018;8:7809.

62. Kurochkin IV, Mizuno Y, Konagaya A, Sakaki Y, Schönbach C, Okazaki Y. Novel peroxisomal protease Tysnd1 processes PTS1- and PTS2-containing enzymes involved in beta-oxidation of fatty acids. *EMBO J*. 2007;26:835-845.

63. Fukuda S, Shimozawa N, Suzuki Y, Zhang Z, Tomatsu S, Tsukamoto T, et al. Human peroxisome assembly factor-2 (PAF-2): a gene responsible for group C peroxisome biogenesis disorder in humans. *Am J Hum Genet.* 1996;59:1210-1220.

64. Chang CC, South S, Warren D, Jones J, Moser AB, Moser HW, et al. Metabolic control of peroxisome abundance. *J Cell Sci*. 1999;112:1579-1590.

65. Imamura A, Shimozawa N, Suzuki Y, Zhang Z, Tsukamoto T, Fujiki Y, et al. Temperature-sensitive mutation of PEX6 in peroxisome biogenesis disorders in complementation group C (CG-C): comparative study of PEX6 and PEX1. *Pediatr Res*. 2000;48:541-545.

66. Berendse K, Ebberink MS, Ijlst L, Poll-The BT, Wanders RJ, Waterham HR. Arginine improves peroxisome functioning in cells from patients with a mild peroxisome biogenesis disorder. *Orphanet J Rare Dis*. 2013;8:138.

67. Sorlin A, Briand G, Cheillan D, Wiedemann A, Montaut-Verient B, Schmitt E, et al. Effect of l-arginine in one patient with peroxisome biogenesis disorder due to PEX12 deficiency. *Neuropediatrics*. 2016;47:179-181.

68. Tanaka AJ, Okumoto K, Tamura S, Abe Y, Hirsch Y, Deng L, et al. A newly identified mutation in the *PEX26* gene is associated with a milder form of Zellweger spectrum disorder. *Cold Spring Harb Mol Case Stud*. 2019;5:a003483.

69. Tran C, Hewson S, Steinberg SJ, Mercimek-Mahmutoglu S. Late-onset Zellweger spectrum disorder caused by PEX6 mutations mimicking X-linked adrenoleukodystrophy. *Pediatr Neurol*. 2014;51:262-265.

70. Maxwell MA, Leane PB, Paton BC, Crane DI. Novel PEX1 coding mutations and 5' UTR regulatory polymorphisms. *Hum Mutat*. 2005;26:279.

71. Yang RY, Quan J, Sondaei R, Aguet F, Segre AV, Allen JA, et al. A systematic survey of human tissue-specific gene expression and splicing reveals new opportunities for therapeutic target identification and evaluation. bioRxiv 311563. doi 10.1101/311563.

72. Kokkinaki M, Sahibzada N, Golestaneh N. Human induced pluripotent stem-derived retinal pigment epithelium (RPE) cells exhibit ion transport, membrane potential, polarized vascular endothelial growth factor secretion, and gene expression pattern similar to native RPE. *Stem Cells*. 2011;29:825-835.

73. Shindou H, Koso H, Sasaki J, Nakanishi H, Sagara H, Nakagawa KM, et al. Docosahexaenoic acid preserves visual function by maintaining correct disc morphology in retinal photoreceptor cells. *J Biol Chem.* 2017;292:12054-12064.

74. Weller S, Gould SJ, Valle D. Peroxisome biogenesis disorders. *Annu Rev Genomics Hum Genet.* 2003;4:165-211.

75. Vasiljevic E, Ye Z, Pavelec DM, Darst BF, Engelman CD, Baker MW. Carrier frequency estimation of Zellweger spectrum disorder using ExAC database and bioinformatics tools. *Genet Med.* 2019;21:1969-1976.

76. Raas-Rothschild A, Wanders RJ, Mooijer PA, Gootjes J, Waterham HR, Gutman A, et al. A PEX6-defective peroxisomal biogenesis disorder with severe phenotype in an infant, versus mild phenotype resembling Usher syndrome in the affected parents. *Am J Hum Genet.* 2002;70:1062-1068.

APPENDIX A

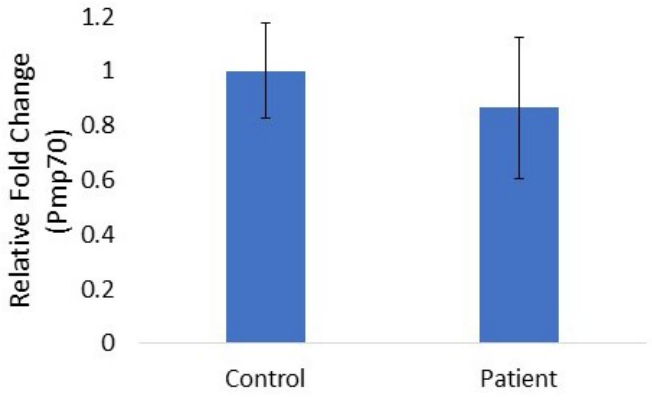

Supplementary Figure 1. Endogenous amounts of Pmp70/ABCD3 protein in skin fibroblast lysates. Levels of Pmp70, a peroxisomal membrane protein involved in lipid transport and a surrogate marker for peroxisome abundance, did not differ significantly between the control and the patient's fibroblasts ($P = 0.50$; n = 3 experimental replicates).